

4

Design of π -Conjugated Systems Using Organophosphorus Building Blocks

Philip W. Dyer and Régis Réau

4.1

Introduction

π -Conjugated oligomers and polymers (Fig. 4.1) have emerged as promising materials for application in flexible, lightweight and low-cost electronic devices such as organic light-emitting diodes (OLEDs) [1], field-effect transistors (FETs), plastic lasers and photovoltaic cells [2]. One of the most appealing attributes of these types of molecular material is their aptitude for exhibiting multifunctional properties, something that is nicely illustrated by their use in the fabrication of high-performance OLEDs, which are employed as devices for flat-panel displays in a host of commercial products (e.g. cell phones, digital cameras) [3]. To achieve an efficient single-layer OLED, in which a π -conjugated system is sandwiched between two electrodes, the organic material has to be able to transport charges and to be highly luminescent [1, 4]. In addition, the molecular material should also (i) be readily processable to give uniform and pinhole-free thin films, (ii) be thermally stable in order to engender durability and (iii) possess an amorphous morphology to prevent light scattering and crystallization-induced degradation. In order to achieve these diverse demands and capabilities from a single material, the only realistic approach is to tailor the properties of π -conjugated oligomers or polymers at the molecular level. Hence the development of advanced organic materials is directly linked to the ability of chemists to fine-tune the properties and the supra-molecular organization of π -conjugated systems. This is possible by exploiting the enormous versatility and scope of organic and organometallic chemistry [1, 2, 5].

To achieve these goals, many different strategies have been used, which include modification of the nature of the conjugated segment itself (topology), introduction of electron-withdrawing or -donating groups and the grafting of bulky or functional side-chain substituents. However, perhaps the most powerful means of influencing and tailoring the physical properties of a material, by way of synthesis, is to vary the chemical composition of the conjugated backbone chain. For example, aromatic five- and six-membered rings have been widely used for the tailoring of π -conjugated systems since their electronic properties (aromatic char-

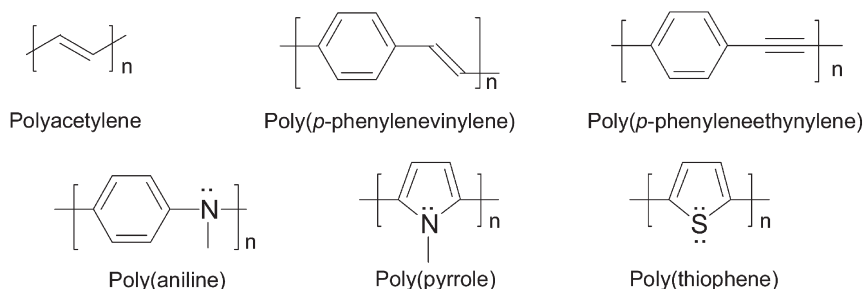


Fig. 4.1 Representative structures of π -conjugated systems.

acter, electron richness/deficiency, polarizability, etc.) can vary considerably according to their structure. Furthermore, these types of ring system provide not only excellent stability, but also offer significant synthetic flexibility: (i) their susceptibility towards electrophilic ring substitution allows for the introduction of pendent substituents with specific electronic and/or steric properties; and (ii) their halogen-substituted derivatives can be utilized in highly versatile catalytic methodologies for C–C bond formation (the so-called Kumada, Stille, Sonogashira, Suzuki–Miyaura and Heck couplings, for example).

Together, these synthetic methods allow for the gram-scale preparation of well-defined and monodisperse conjugated materials, in ways that allow for the control of both regio- and stereochemistry. This synthetic flexibility is crucial in allowing a reliable correlation of structure and properties to be established, via the synthesis of oligomers with increasing chain length and hence the optimization of the desired physical properties. However, each class of building block has its own advantages and disadvantages. One potential drawback of these types of five- and six-membered ring units is that their relatively high aromatic character results in a competition between π -electron confinement within the ring and delocalization along the conjugated chain [5d, 6]. This point reveals the possible conflicting properties of a given building block: although aromaticity provides stability and ease of functionalization, it can hinder access to low HOMO–LUMO gap materials.

The types of coupling methodology described above potentially allow for the preparation of a broad range of homo- and mixed oligomers and polymers with considerable structural variation. However, it is amazing to note that only a limited number of basic building blocks are commonly used, namely olefins, acetylenes, aromatic rings (benzene, naphthalene, etc.) and heterocyclopentadienes (thiophene, pyrrole, etc.) (Fig. 4.1) [1–5]. Hence the introduction of novel building blocks is clearly a basis for the further tailoring of π -conjugated systems. Of course, the challenge is not just simply to prepare new series of conjugated materials, but to introduce synthons that exhibit properties that the already well-established building blocks do not possess, in order to obtain innovative molecular architectures or unique electronic properties.

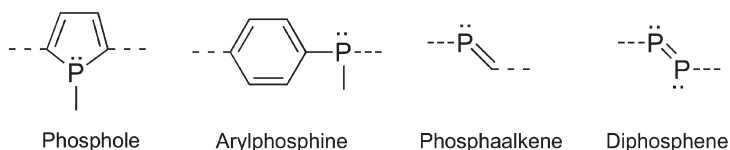


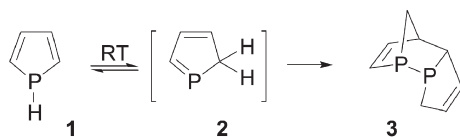
Fig. 4.2 P-based building blocks used for the construction of π -conjugated systems.

In contrast to sulfur- and nitrogen-based ring systems, which have been widely exploited for decades (Fig. 4.1), phosphorus-derived building blocks (Fig. 4.2) have only emerged in the late 1990s for the construction of π -conjugated materials [5j]. This situation is very surprising considering that the chemistry of these P-containing moieties is now well developed and that they exhibit properties that are markedly different from those of their N analogs [7]. This chapter intends to give an overview of the synthesis of various classes of π -conjugated oligomers and polymers incorporating P moieties (Fig. 4.2) and to illustrate the conceptual design and specific properties that result directly from the presence of the P atom. The presentation will follow a largely chronological order starting with phosphole (Fig. 4.2), which is still the most extensively used P unit for the synthesis of conjugated materials. Note that polyphosphazenes [8], which are the most familiar synthetic polymers incorporating phosphorus, will not be included in this review since they do not display the type of extended π -conjugation as sought in systems presented in Figs. 4.1 and 4.2.

4.2

Phosphole-containing π -Conjugated Systems

The first phospholes were described in the 1950s [9a–c], but synthetic methods combining high yields and diversity of substitution pattern were only discovered in the late 1960s [10a]. Hence the chemistry of phospholes is in its infancy compared with that of pyrrole and thiophene, compounds that were discovered during the 19th century. This is illustrated by the fact that the parent phosphole **1** (Scheme 4.1) was only characterized by NMR spectroscopy as recently as 1983 [10b]. Today, however, the chemistry (synthesis, reactivity, coordination behavior, etc.) of this P-based heterocycle has reached a much more mature state, allowing its use as a building block for the engineering of π -conjugated materials to be envisaged.



Scheme 4.1

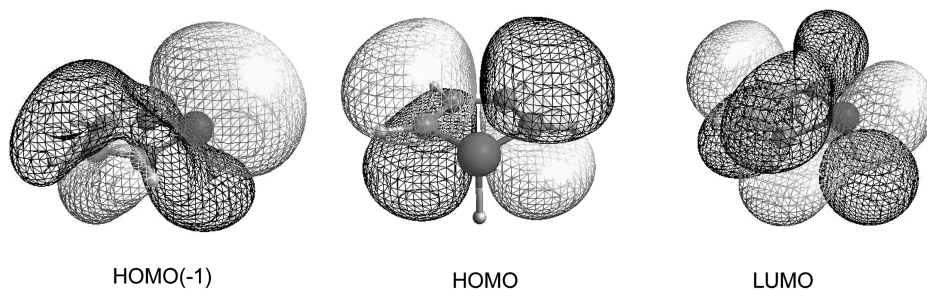


Fig. 4.3 B3LYP/6-31G⁺⁺ HOMO(-1), HOMO and LUMO of parent phosphole.

One of the major issues in understanding the properties of the phosphole ring was to determine its degree of aromaticity. This problem has long been debated and it is now accepted that, in marked contrast to pyrrole, phosphole exhibits a weak aromatic character [7, 11]. For example, the calculated aromatic stabilization energy (ASE) and nucleus-independent chemical shift (NICS) values are 7.0 kcal mol⁻¹ and -5.3 for phosphole compared with 25.5 kcal mol⁻¹ and -15.1 for pyrrole [11]. This lack of aromaticity is a consequence of two intrinsic properties of phospholes: the tricoordinate P atom adopts a pyramidal geometry and its lone pair exhibits a high degree of s character (Fig. 4.3). Together these two features prevent efficient interaction of the P lone pair with the endocyclic π -system. Although calculations have shown that planar phosphole would be more aromatic than pyrrole, this stabilization is not sufficient to overcome the high planarization barrier of the P atom (35 kcal mol⁻¹) [12], but is responsible for the reduced P-inversion barrier in phosphole (ca. 16 versus 36 kcal mol⁻¹ for phospholanes [12a]). In fact, the weak aromatic character of the phosphole ring is due to hyperconjugation involving the exocyclic P-R σ -bond and the π -system of the dienic moiety [13]. As proposed for siloles (the heterole containing a tetrahedral Si center), which exhibit a similar σ - π interaction [14], this hyperconjugation is possible since the P atom adopts a tetrahedral geometry and the exocyclic P-R bonds are relatively weak.

These electronic properties (low aromatic character, σ - π hyperconjugation), which set phosphole apart from pyrrole and thiophene, have very important consequences. First, phosphole does not undergo electrophilic substitution, but does possess a reactive heteroatom. As a result, an electrophile will not attack the heteroatom C- α carbon atom, as observed with pyrrole, but the P atom instead (Fig. 4.4). Hence this P-containing ring has its own chemistry (synthetic routes, methods of functionalization, etc.) that cannot be predicted by simply extrapolating that of its aromatic S and N analogs. Second, phospholes make appealing building blocks for the tailoring of conjugated systems, since it is well established that conjugation will be enhanced for macromolecules built from monomer units that exhibit low resonance energies [5d, 6]. This phenomenon is nicely illustrated by theoretical work that showed that the energy gaps of oligo(phosphole)s are signif-

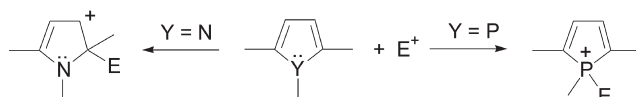


Fig. 4.4 Reactivity of pyrrole and phosphole towards electrophiles.

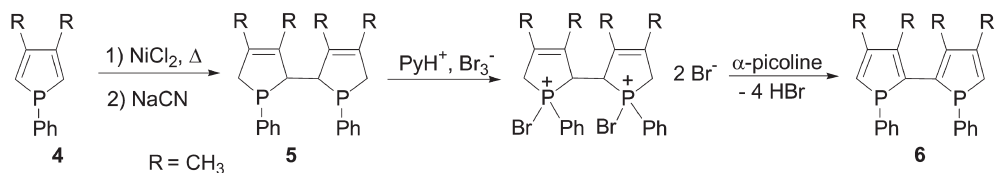
icantly lower than those of the corresponding oligo(pyrrole)s or oligo(thiophene)s [6]. Furthermore, the ease of functionalization of the P atom offers a unique way of creating structural diversity, including the preparation of transition metal complexes, from a single precursor. Lastly, if the chemistry of siloles is taken as a source of inspiration [14], the σ - π hyperconjugation associated with the phosphole ring should allow for the synthesis of multidimensional systems exhibiting σ - π conjugation (so-called “through-bond delocalization”). It will be demonstrated that all three of these features, which thiophene or pyrrole cannot offer, have been fully exploited in recent years for the preparation of phosphole-containing conjugated oligomers and polymers.

A last important issue that is crucial for the development of phospholes as building blocks for materials is their thermal stability and, to a lesser extent, their ease of handling and manipulation. The parent phosphole **1** can be observed at $-100\text{ }^\circ\text{C}$; however, at room temperature, it isomerizes via a [1, 5]-sigmatropic shift to the 2*H*-phosphole **2**, which rapidly dimerizes to afford the endo derivative **3** (Scheme 4.1) [10]. The thermal stability of phospholes is considerably increased by the introduction of substituents on the ring. In particular, the nature of the P substituent has a dramatic influence since it is this group that migrates giving rise to the unstable 2*H*-phosphole **2** (Scheme 4.1). For example, phospholes bearing phenyl, cyclohexyl, cyano or alkoxy substituents at phosphorus are all stable at room temperature. Indeed, the decomposition temperatures of 2,5-diaryl-*P*-phenylphospholes, as estimated by thermogravimetric analyses, can reach $200\text{ }^\circ\text{C}$ [15a]. Furthermore, these *P*-phenylphospholes are not moisture sensitive and can be purified by standard methods. In contrast, although *P*-amino- and *P*-halophospholes can be obtained at room temperature, they are readily hydrolyzed [15]. Just as for classical phosphines, phospholes have to be handled under an inert atmosphere in order to avoid oxidation of the P center. Notably, however, 2,5-diarylphospholes are generally stable enough to be purified and manipulated under air [15a].

4.2.1

α,α' -Oligo(phospholes)

When considering the synthesis of phospholes, one has to forget most of the classical and powerful methods employed for the preparation of thiophenes and pyrroles. For example, Paal–Knorr condensation, direct *ortho*-lithiation, halogenation with NBS or $\text{I}_2/\text{Hg}^{2+}$ and Vilsmeier–Haack formylation are not operative in phosphole chemistry. Likewise, no chemical or electrochemical oxidative polymerization

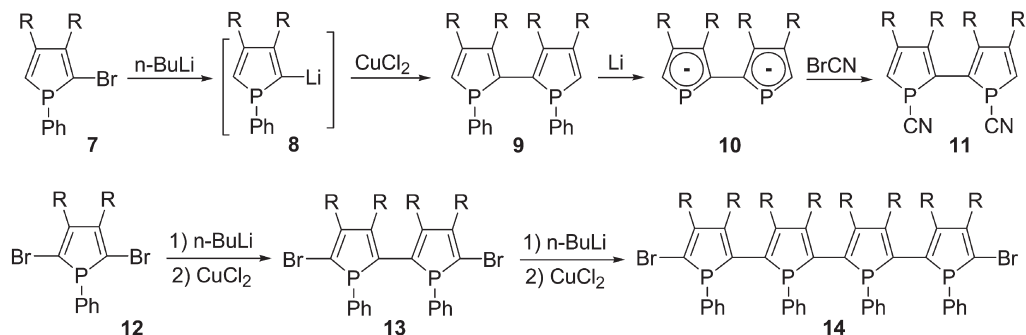


Scheme 4.2

of phospholes has yet been achieved. As a result, the preparation of α,α' -oligo (phosphole)s is a real synthetic challenge.

Mathey's group achieved a breakthrough in this field in the 1990s with the discovery of several synthetic routes to linear bi- and quaterphospholes. Initially, non-capped 2,2'-biphosphole **6** was prepared via a four-step sequence from 1-phenyl-3,4-dimethylphosphole **4** (Scheme 4.2), a starting material that is readily accessible in multi-gram quantities [16]. The Ni(II)-promoted reductive dimerization of phosphole **4**, followed by decomplexation, afforded the di-2-phospholene **5** (Scheme 4.2) [17]. Successive *P*-bromination and dehydrohalogenation gave rise to the target 2,2'-biphosphole **6**, which is stable enough to be purified by column chromatography [18a]. It is obtained as a mixture of diastereoisomers owing to the presence of two chirogenic P centers, which are in rapid equilibrium at room temperature since the barrier to inversion at phosphorus is low (ca. 16–17 kcal mol⁻¹) owing to the aromatic character of the planar transition state [18].

The second route to oligo(phosphole)s is based on the formation of 2-lithiophospholes. This reaction was a landmark in this area since it provided the first direct means of functionalization of the phosphole ring and opens the way to metal-catalyzed coupling reactions [19]. A quantitative bromine–lithium exchange transforms the 2-bromophospholes **7** into their highly reactive 2-lithio analogs **8** (Scheme 4.3). These 2-lithiophospholes undergo oxidative coupling leading to bipospholes **9** upon addition of copper(II) chloride (Scheme 4.3)



7-9, 12-13: R = CH₃, Ph; 10, 11, 14 : R = CH₃

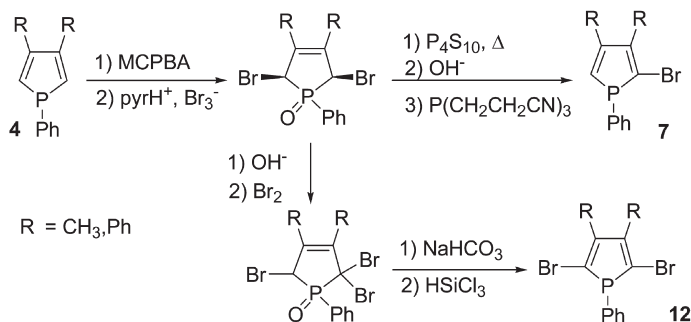
Scheme 4.3

[19, 20]. The nature of the P substituents of **9** can be readily varied via a two-step sequence involving the generation of the phospholyl anion **10** by reductive cleavage of the exocyclic P–C bonds with lithium (Scheme 4.3). The dianion **10** can act as a nucleophilic reagent in the synthesis of new biphospholes, as illustrated with the preparation of **11** (Scheme 4.3) [18b]. The very efficient bromine–lithium exchange methodology has also been applied to the preparation of bromo-capped biphosphole **13** and quarterphosphole **14** using the dibromo precursor **12** (Scheme 4.3) [21]. These oligo(phosphole)s are obtained in good yields (e.g. **12** \rightarrow **14**, 55%) as mixtures of diastereoisomers.

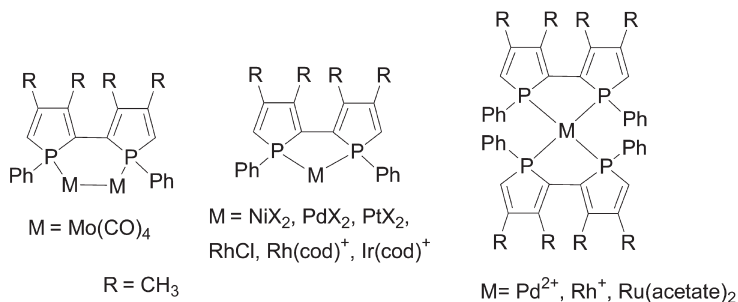
This expedient and efficient synthetic methodology seems very attractive for the construction of longer, well-defined oligomers since **13** and **14** bear reactive termini. However, **14** is still the longest oligo(phosphole) known to date. No iterative coupling study has been undertaken, presumably because the preparation of the starting bromo precursors **7** and **12** is laborious and time consuming (Scheme 4.4) [19, 21], since it has been proved impossible to perform one-step bromination of the phosphole ring.

Unfortunately, the optical and electrochemical properties of these linear phosphole oligomers have not yet been elucidated, precluding an interesting comparison with related oligo(pyrrole)s. However, oligo(phosphole)s **9** ($R = \text{CH}_3$), **11** and **14** (Scheme 4.3) have been characterized by X-ray diffraction studies, which does give some insight into the properties of these systems.

In all cases, the phosphorus atoms of **9**, **11** and **14** adopt a pyramidal geometry, with the endocyclic P–C bond distances consistent with single bonds. Together, these geometric data show that, as observed for monophospholes, the P lone pair is not conjugated with the endocyclic diene framework. Furthermore, solid-state studies also revealed that the heterocyclic phosphole units are not coplanar. The dihedral angle between the two phosphole rings in **9** and **11** is about 46° [18b,c], whereas in **14** the twist angle between the two inner rings is 25.1° and that between the outer pair is 49.7° [21]. These rotational distortions should preclude these oligo(phosphole)s from possessing extended π -conjugated systems. However, these twists are probably due to packing effects in the solid state since the color of these compounds varies from pale yellow (**9**, **11**) to



Scheme 4.4



Scheme 4.5

deep orange (**14**), suggesting rather high λ_{max} values and, consequently, low optical HOMO–LUMO band gaps. The red shift observed on going from derivatives **9** and **11** to **14** hints that, in line with theoretical studies [6b,c], the energy gap of oligo(phosphole)s decreases with increasing chain length.

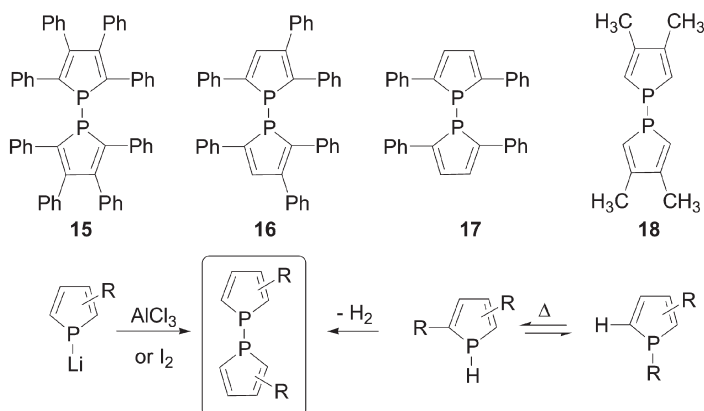
It is noteworthy that the P atoms of these phosphole oligomers retain the versatile reactivity observed with monophospholes [7]. In particular, bisphosphole **9** exhibits a rich coordination chemistry, which allows for the preparation of a variety of neutral and cationic transition metal complexes (Scheme 4.5) [18a,b, 22]. These have been used as precursors for homogeneous catalysts [22]; however, their photophysical properties have not been studied.

It can be concluded that the size of the family of linear oligo(phosphole)s is somewhat limited to bi- and tetramers to date, although longer derivatives are potentially accessible via the efficient synthetic routes developed by Mathey's group. The synthesis of other oligo(phosphole)s and the elucidation of their photo-physical and electrochemical properties are still needed in order to establish reliable structure–property relationships.

4.2.2

Derivatives Based on 1,1'-Biphosphole Units

The α,α' -oligo(phosphole)s described in the previous section possess classical one-dimensional conjugated systems based on alternating double and single C–C bonds. The use of phospholes as building blocks allows for the variation in the topology of the conjugation pathway through the synthesis of 1,1'-biphospholes (Scheme 4.6). These derivatives date back to the early days of phosphole chemistry, the first member of the family having been prepared in 1979 (**15**, Scheme 4.6) [23a], with the three other examples **16–18** appearing in the early 1980s [23b,d]. The most common synthetic routes to 1,1'-diphospholes involve either the oxidative coupling of readily available phospholyl anions [23d] or the thermolysis of phospholes (Scheme 4.6). This last route implies the formation of transient P–H phospholes, via 1,5-shifts of R and H, followed by loss of H_2 via an as yet unexplained mechanism [10c, 23d]. The P atoms of 1,1'-biphospholes



Scheme 4.6

retain a pyramidal shape, as observed for the corresponding monomeric phospholes [23e].

1,1'-Biphospholes have been mainly used as precursors for the synthesis of other P-containing species including mono- and diphosphaferrocenes [24]. Their electronic properties were recently investigated [25] with the aim of trying to observe any interaction between the π -systems via the P–P linkage resulting from the σ – π hyperconjugation occurring within the phosphole ring (Fig. 4.3). The fact that π -chromophores can effectively be conjugated via σ -skeletons [26], especially those exhibiting high polarizability and low σ – σ^* energy gaps, was recognized by Hoffmann et al. in the late 1960s [26a,b]. This unusual conjugation pathway results in novel electronic properties that are starting to be exploited in materials science. For example, in oligo(1,1'-siloles) an effective interaction (σ^* – π^* conjugation) occurs between the Si–Si bridges and the butadienic moieties [27a,b], making these macromolecules very attractive chemical sensors for aromatic substrates [27c,d,g] and highly efficient electron-transporting materials for light-emitting diode materials [27e,f].

With a view to further exploitation of these unusual σ – π conjugated species, the mixed thiophene–phosphole derivative **19** (Fig. 4.5) has been prepared from the corresponding monomeric phospholyl anion as an air-stable powder [25]. As expected, theoretical calculations and UV–Vis data clearly establish a through-bond electronic interaction between the two 2,5-dithienylphospholyl moieties via the P–P bridge. One important consequence of this σ – π conjugation is that **19** possesses a smaller optical HOMO–LUMO gap than the corresponding 2,5-dithienylphosphole (see Section 4.2.3). It is interesting that the P atoms of **19** are reactive, allowing further chemical modification of the nature of the P–P bridge. Derivatives **20** and **21** are readily obtained using classical reactions, which exploit the nucleophilic behavior of the σ^3, λ^3 -P centers of **19** (Fig. 4.5). These chemical modifications have an impact on the optical properties of the assemblies. For example, oxidation of one P center or complexation of the P atoms

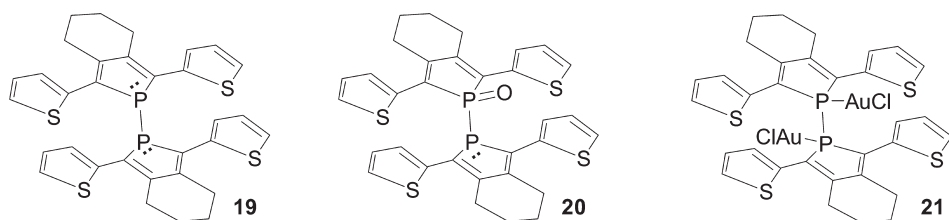
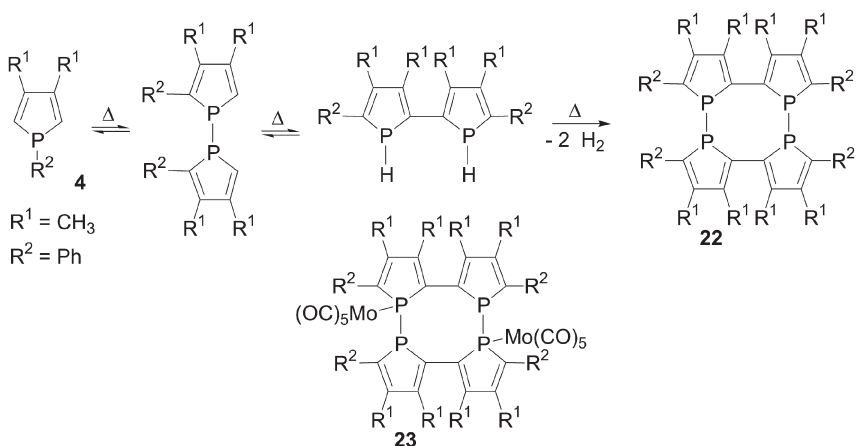


Fig. 4.5 Structures of thienyl-capped 1,1'-biphospholes and Au(I) derivatives.

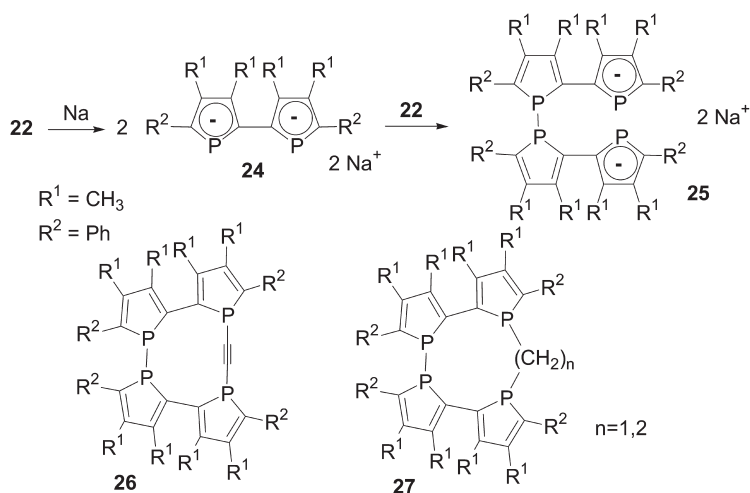
with gold(I) results in bathochromic shifts of the band onset compared with 1,1'-biphosphole **19** [25].

The second route to 1,1'-diphospholes, involving [1, 5]-sigmatropic shifts and loss of H₂ (Scheme 4.6), conducted with 1-phenylphosphole **4**, afforded the macrocycle **22** (Scheme 4.7) [28a]. This compound has a remarkable structure with two α,α' -biphosphole cores connected by two P–P bonds. An X-ray diffraction study revealed that the P atoms are located trans with respect to the linking C–C bond [28b]. However, **22** is very probably flexible since, in the corresponding Mo(CO)₅ complex **23** (Scheme 4.7), they adopt mutually cis positions [28a]. As observed in the linear series, the two P rings of the α,α' -biphosphole moieties of **22** are not coplanar (twist angle, 44.2°) [28b]. The UV–Vis data for this unique type of macrocycle have not been reported, but its red color again suggests a low HOMO–LUMO separation due to σ – π conjugation.

Significantly, derivative **22** can be used as a precursor to other macrocycles featuring the 1,1'-diphosphole moiety. For example, the reductive cleavage of the two P–P bonds with sodium gave the dianion **24**, which, upon reaction with **22**, afforded the dianion **25** (Scheme 4.8) [28c]. Derivative **25** is a versatile nucleophile that reacts with tetrachloroethylene and dihaloalkanes to give the novel macro-



Scheme 4.7



Scheme 4.8

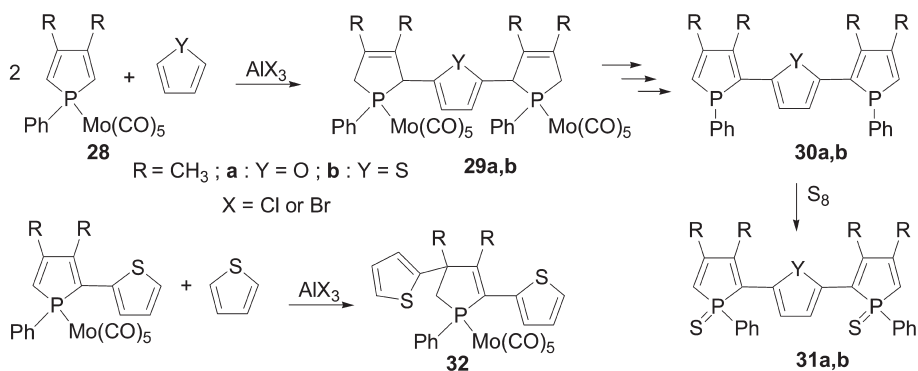
cycles **26** and **27**, respectively [28c]. Compound **26** was characterized by an X-ray diffraction study [28c], which revealed that this fairly rigid 10-membered macrocyclic compound exhibits some strain, as shown by the nonlinearity of the $\text{P}-\text{C}\equiv\text{C}-\text{P}$ unit [$\text{P}-\text{C}-\text{C}$, $170.2(8)^\circ$ and $173.5(6)^\circ$].

The above-mentioned examples nicely illustrate the diversity of structures offered through the use of 1,1'-diphosphole building blocks. Importantly, it has been shown that these moieties exhibit σ - π conjugation, a type of electronic interaction that is still relatively rare. Together, these results show that this type of P-based moiety is a promising elementary unit for the engineering of conjugated systems.

4.2.3

Mixed Oligomers Based on Phospholes with Other (Hetero)aromatics

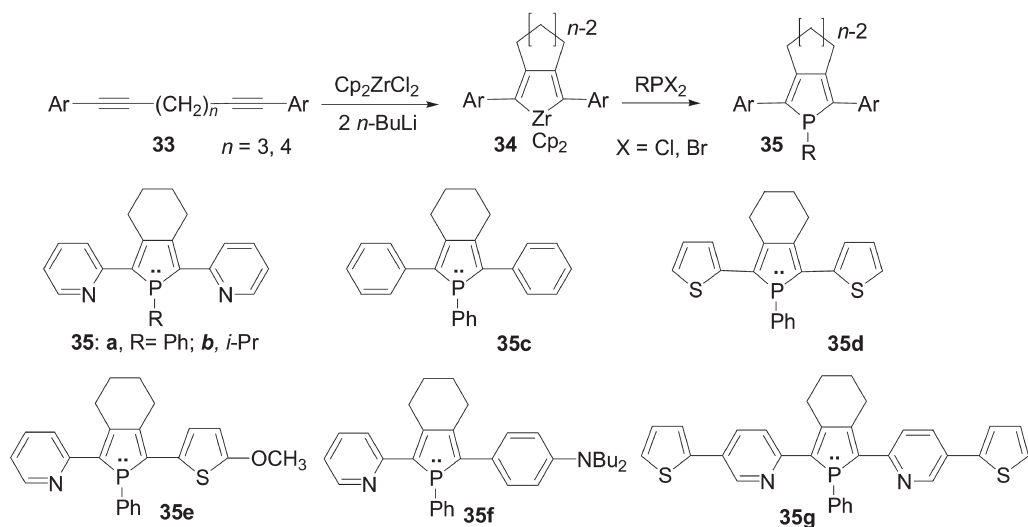
The first series of mixed macromolecules based on phospholes and other (hetero)-aromatics to be prepared were composed of 2,5-di(2-phosphole)thiophene or -furan derivatives. The key step in their synthesis is an electrophilic substitution in which the protected phosphole **28** acts as an electrophile towards electron-rich thiophene or furan rings, leading to the 3-phosphole adducts **29a,b** (Scheme 4.9) [29a]. These compounds were then transformed into the corresponding σ^3,λ^3 -phosphole derivatives **30a,b** through a classical deprotection-bromination-dehydrohalogenation sequence (Scheme 4.9) [29]. Although these macromolecules evidently absorb in the visible region (**30a**, orange; **30b**, bright yellow), no UV-Vis data are available. An X-ray diffraction study performed on thioxo derivative **31b** showed that only one phosphole ring is coplanar with the central furan unit (twist angle, 3.3 ± 0.1 and $40.1 \pm 0.1^\circ$). The two inter-ring C-C bond dis-



Scheme 4.9

tances [1.452(4) and 1.461(6) Å] lie between those observed for C–C single and double bonds, a feature that is in favor of a certain degree of delocalization [29a].

The first systematic investigation of phosphole-containing conjugated polymers systems, which starts with model molecules and builds up to conductive polymers and materials suitable for OLED applications, was undertaken with 2,5-di(heteroaryl)-phospholes. In contrast, these derivatives are not accessible by the electrophilic substitution route described above for the preparation of **30**, since the second condensation step gives rise to 2,4-dithienylphospholene **32** (Scheme 4.9) [29a]. However, 2,5-di(heteroaryl)phospholes are readily accessible via a widely applicable organometallic route known as the Fagan–Nugent method [30]. The key to obtaining the desired 2,5-substitution pattern is to perform the metal-mediated oxidative coupling of diynes **33** possessing a $(\text{CH}_2)_3$ or a $(\text{CH}_2)_4$ spacer (Scheme 4.10) [15a, 31]. These diynes, including unsymmetrical variants, can be readily prepared using Sonogashira coupling [15a, 31]. The zirconacyclopentadiene intermediates **34** are extremely air and moisture sensitive derivatives that react with dihalophosphines to give the corresponding phospholes **35a–g** in medium to good yields (Scheme 4.10). This route is highly flexible since it not only allows electron-deficient and electron-rich rings to be introduced in the 2,5-positions, but also permits the nature of the P substituent to be varied. For example, the σ^3, λ^3 -phospholes **35a** [31a] and **35d** [31b] bearing electron-deficient and electron-rich substituents, respectively, have been prepared using this approach. Together with the $\text{W}(\text{CO})_5$ -complex of **35g** [31b], they were subsequently characterized by X-ray diffraction studies. In spite of the different natures of the two 2,5-substituents (electronic disparity, shape, etc.), these compounds share some important structural features in the solid state. The twist angles between two adjacent rings are rather small [**35a**, 7.0 and 25.6°; **35d**, 12.5 and 16.7°] and the phosphorus atoms are strongly pyramidalized, as indicated by the sum of the CPC angles [**35a**, 299.3°; **35d**, 299.3°]. Note that these derivatives are the first phosphole-based conjugated systems that are planar in the solid state. The lengths of the C–C linkages between the rings [1.436(6)–1.467(8) Å] are in the range expected for $\text{Csp}^2\text{–Csp}^2$



Scheme 4.10

single bonds. Together these metric data suggest a delocalization of the π -system over the three heterocycles.

In solution, phospholes **35a–g** present broad absorptions in the visible region of the spectrum attributed to π - π^* transitions [15a, 31]. The values of λ_{max} and the optical end absorption λ_{onset} depend on the nature of both the P and the 2,5-substituents. A red shift of the values of λ_{max} for *P*-arylphospholes is observed relative to those of the corresponding *P*-alkyl analogs (Table 4.1, **35a** vs. **35b**). An important bathochromic shift was recorded on replacing the phenyl groups either by 2-pyridyl ($\lambda_{\text{max}} = 3 \text{ nm}$) or 2-thienyl rings ($\lambda_{\text{max}} = 58 \text{ nm}$) (Table 4.1) [15a]. Collectively, these data suggest that the HOMO–LUMO gap gradually decreases in the series **35c** < **35a** < **35d**, a feature that was confirmed by high-level theoretical calculations [15a]. This variation was initially attributed to the fact that phospholes possess low-lying LUMO levels (high electron affinity), which favors intramolecular charge transfer from the electron-rich thienyl substituents [15a]. A more recent theoretical study proposed that the more pronounced π -conjugation in **35d** is due to a better interaction between the HOMO of the phosphole with the HOMO of the thiophene compared with that with pyridine [32]. It is interesting that the value of λ_{max} recorded for **35d** (412 nm) is considerably more red shifted than those of related 2,5-dithienyl-substituted pyrrole (322 nm), furan (366 nm) or thiophene (355 nm) [33]. These observations help to establish phospholes as valuable building blocks for the construction of co-oligomers exhibiting low HOMO–LUMO separations. This appealing property is probably due to the weak aromaticity of the phosphole ring, which favors an exocyclic delocalization of the dienic π -electrons.

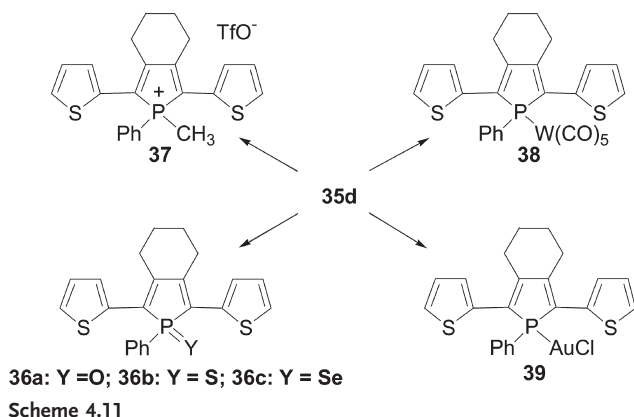
Table 4.1 Physical properties of di(heteroaryl)phospholes **35a–d** and derivatives **36b** and **37–39**

Compound	$\lambda_{\text{max}}^{[a]}$ (nm)	$\lambda_{\text{onset}}^{[a]}$ (nm)	Log ϵ	$\lambda_{\text{em}}^{[a]}$ (nm)	Φ_f	$E_{\text{pa}}^{[b]}$ (V)	$E_{\text{pc}}^{[b]}$ (V)
35a	390	448	4.02	463	1.1×10^{-2}	+0.83	-2.45
35b	371	430	4.10	458	–	+0.79	-2.67
35c	354	430	4.20	466	14.3×10^{-2}	+0.69	-2.88
35d	412	468	3.93	501	5.0×10^{-2}	+0.40	–
36b	432	496	3.98	548	4.6×10^{-2}	+0.68	-1.95
37	442	528	3.92	593	0.8×10^{-2}	+0.92	-1.66
38	408	475	4.04	506	1.3×10^{-2}	+0.70	-2.20
39	428	500	4.18	544	14.0×10^{-2}	+0.82	-1.75

^[a] In THF.^[b] In CH_2Cl_2 , referenced to ferrocene/ferrocenium half-cell.

Varying the nature of the 2,5-substituents is also an effective way of tuning the emission and electrochemical behavior of phosphole-based extended π -electron systems. For example, di(2-pyridyl)phosphole **35a** emits blue light, whereas the emission of di(2-thienyl)phosphole **35d** is red shifted (Table 4.1). Note that the quantum yields in solution are relatively low, the highest (14.3×10^{-2}) being observed for 2,5-diphenylphosphole **35c** (Table 4.1). All the σ^3 -phospholes **35** show redox processes that are irreversible at 200 mV s^{-1} [15a], with the redox potentials being related to the electronic properties of the phosphole substituents (Table 4.1). For example, derivative **35d** featuring electron-rich thienyl substituents is more easily oxidized than compound **35a**, which bears electron-deficient pyridyl groups.

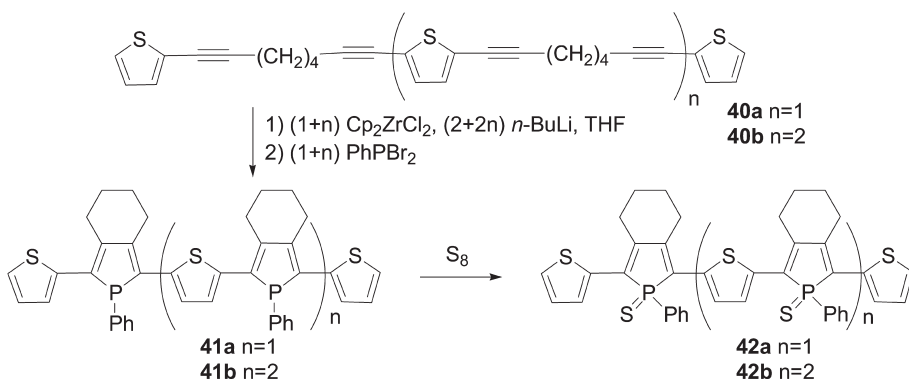
One of the appealing properties of phosphole rings when creating structural diversity in these types of system is the versatile reactivity of the endocyclic heteroatom. Exploiting the nucleophilic behavior of the P center allows direct access to a range of new π -conjugated systems, including metal complexes, as illustrated with dithienylphosphole **35d** (Scheme 4.11). It is noteworthy that the bis(2-thienyl)phosphole moiety remains almost planar in the coordination sphere of $\text{W}(\text{CO})_5$ (twist angles, 7.3 and 13.4°) and AuCl (twist angles, 3.8 and 13.5°) and that the bond lengths and angles are unchanged upon coordination [15a, 34]. However, these chemical modifications of the nucleophilic P center have a profound impact on the optical and electrochemical properties of the phosphole oligomers as a whole. For example, on going from the σ^3 -phosphole **35d** to the neutral σ^4 -derivative **36b** and the σ^4 -phospholium salt **37**, a red shift is observed in their UV-Vis spectra, together with an increase and decrease in their oxidation and reduction potentials, respectively (Table 4.1). These trends can be rationalized on the basis that within this series the electronic deficiency of the P atom is gradually augmented [15a, 32]. Exploitation of this method of tailoring π -conjugated



systems, which is simply not possible with pyrrole and thiophene units, has led to the optimization of the properties of thiophene–phosphole co-oligomers for use as materials suitable for OLED fabrication.

Single-layer OLEDs have been prepared through sublimation of the thermally stable thioxo derivative **36b** and gold complex **39** on to semi-transparent indium–tin oxide (ITO) anodes, with both substrates forming homogeneous thin films [34]. In contrast, the o^3 -phosphole **35d** decomposed under sublimation conditions. The device prepared using **36b** as the active organic layer exhibited yellow emission for a relatively low turn-on voltage of 2 V. The electroluminescence (EL) spectra of this device match those of the solid-state photoluminescence (PL) of **36b**, showing that the source of the EL emission band is from the phosphole derivative. In contrast, the emission exhibited by the single-layer device constructed using gold complex **39** covers the 480–800-nm region [34]. The low-energy emissions are probably due to aggregate formation in the solid state. It is clear that the gold centers play a key role in the formation of these aggregates, probably via auriphilic interactions [35], since no low-energy luminescence bands are observed with the thioxophosphole derivatives **36b**. The comparatively low maximum brightness (ca. 3613 cd m^{-2}) and EL quantum yields (ca. 0.16%) of the single-layer OLEDs can be increased by nearly one order of magnitude by using a more advanced device, in which the organic layer consisting of **36b** or **39** was sandwiched between hole- and electron-transporting layers (α -NPD and Alq₃, respectively) [34].

Another effective way to further improve OLED performance and also to tune their color is to dope highly fluorescent dyes as guests into an emissive host matrix [36]. With this in mind, thioxophosphole **36b** was evaluated as a host material for DCJTB, the best red-emitting dopant for OLEDs reported to date [1d]. This device showed red emission from DCJTB, with an EL of 1.83% and a maximum brightness of ca. $37\,000 \text{ cd m}^{-2}$ [34]. Notably, the external EL quantum efficiency of this device is unaffected by drive current density in the range $0\text{--}90 \text{ mA cm}^{-2}$ [34]. This behavior is very promising since the efficiency of DCJTB-doped Alq₃



Scheme 4.12

devices usually decreases rapidly with the driving current, something that results from quenching effects of charged excited states of Alq_3 on the red dopants [36].

The evolution of optical and electrochemical properties with increasing chain length has been investigated for α, α' -thiophene–phosphole (Th-Phos) oligomers in order to gain a greater understanding of the characteristics of these novel π -conjugated systems. To this end, the well-defined oligomers **41a,b** were prepared using the Fagan–Nugent method from the corresponding bis- and tris-diynes **40a,b** (Scheme 4.12) [37]. Derivatives **41a,b**, and also their thiooxo-derivatives **42a,b**, exist as a mixture of diastereoisomers due to the presence of stereogenic P centers. They are air stable and soluble in common organic solvents (e.g. THF, CH_2Cl_2). Significantly, however, the yields of the various oligomers decrease dramatically with increasing chain length (Table 4.2), precluding the preparation of longer chain derivatives.

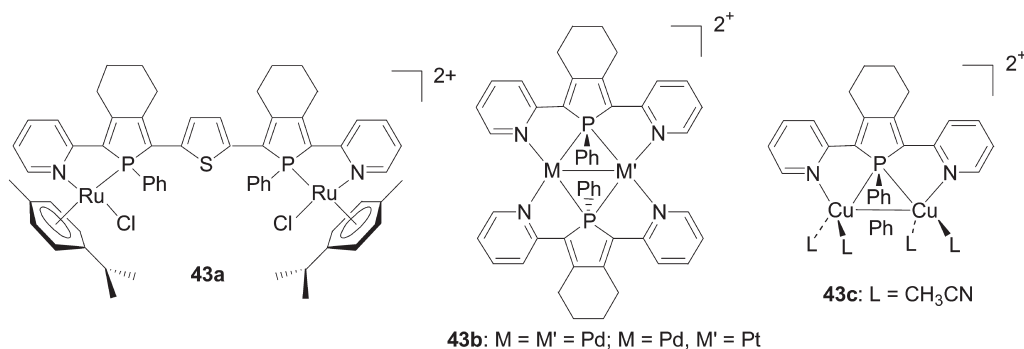
With respect to their electronic properties, the longest wavelength absorption, emission band and the oxidation potentials all gradually shift to lower energies with increasing chain length (Table 4.2). This reflects the expected decrease in the HOMO–LUMO gap upon increasing the chain length of the α, α' -(thio-

Table 4.2 Preparation and physical properties of oligo(α, α' -thiophene–thioxophosphole)s

Compound	Yield (%)	$\lambda_{\text{max}}^{[a]}$ (nm)	$\lambda_{\text{onset}}^{[a]}$ (nm)	Log ϵ	$\lambda_{\text{em}}^{[a]}$ (nm)	$E_{\text{pa}}^{[b]}$ (V)
36b ($n = 0$)	93	432	496	3.98	548	+0.68
42a ($n = 1$)	78	508	590	4.26	615	+0.45
42b ($n = 2$)	32	550	665	4.42	–	–

^[a] In THF.

^[b] In CH_2Cl_2 , referenced to ferrocene/ferrocenium half-cell.



Scheme 4.13

phene–phosphole) oligomers. It is therefore likely that the effective conjugation pathlength is much longer than 7 units for oligomers of these types. Notably, the value of λ_{max} for Th(Phos-Th)₂ **41a** (490 nm) is considerably red shifted compared with that of quinquethiophene (ca. 418 nm) [38], once again showing that replacing a thiophene subunit by a phosphole ring induces an important decrease in the optical HOMO–LUMO gap. It is also noteworthy that oligo(α,α' -thiophene–phosphole)s **42a,b** incorporating σ^4 -thioxophospholes have smaller HOMO–LUMO gaps relative to their precursors **41a,b** based on σ^3 -P rings. These results, along with the good stability and solubility of derivatives **41a,b** and **42a,b**, should encourage the search for new synthetic routes to longer oligo(α,α' -thiophene–phosphole)s.

The coordination of π -chromophores to transition metals is a powerful way to modify their characteristics and to engender novel properties. Two remarkable examples of this methodology are the use of cyclometalated (phenylpyridinato)Ir(II) complexes (highly efficient phosphorescent dopants for OLEDs due to the strong spin–orbit coupling caused by the heavy metal ion) [4d, 39] and homoleptic (aminostyrylbipyridine)Ru(II) complexes (powerful octupolar NLO-phores due to the octahedral geometry of the metal center) [40]. Since 2-pyridylphosphole moieties can act as 1,4-chelates towards transition metals, as illustrated with the synthesis of complexes **43a–c** (Scheme 4.13), it was of interest to examine the behavior of these conjugated P-containing oligomers in a similar way [41]. The UV–Vis spectrum of the free ligand and of the Ru(II) complex are almost identical [41a]. In contrast, for the Pd(I) dimer, low-energy UV–Vis absorptions assigned to charge transfer from the phosphorus–metal fragment to the pyridine ligands were observed [41c].

One key property of pyridylphosphole ligands is their heteroditopic nature. They possess two coordination centers with different stereo-electronic properties, which, in accordance with Pearson's antisymbiotic effect [42a], can control the orientation of a second chelating ligand in the coordination sphere of a square-planar d^8 -metal center [42b]. This property has been exploited in order to control the in-plane parallel arrangement of 1D-dipolar chromophores [42d]. Phospholes



Scheme 4.14

35e,f (Scheme 4.14) have a typical “D-(π -bridge)-A” dipolar topology. They exhibit only moderate NLO activities ($\beta_{1.9 \mu\text{m}}$, ca. 30×10^{-30} esu), something probably due to the weak acceptor character of the pyridine group [42d]. However, the potential of these dipoles in NLO is considerably increased by their P,N-chelate behavior. In accordance with the antisymbiotic effect, they undergo stereoselective coordination leading to a close parallel alignment of the dipoles on the square-planar d^8 Pd(II) template. Thus, the trans-effect can overcome the natural anti-parallel alignment tendency of 1D-dipolar chromophores at the molecular level. The non-centrosymmetric complexes **44e,f** exhibit fairly high NLO activities ($\beta_{1.9 \mu\text{m}}$, ca. $170\text{--}180 \times 10^{-30}$ esu), something that is probably due to the onset of ligand-to-metal-to-ligand charge transfer, which contributes coherently to the second harmonic generation [42d].

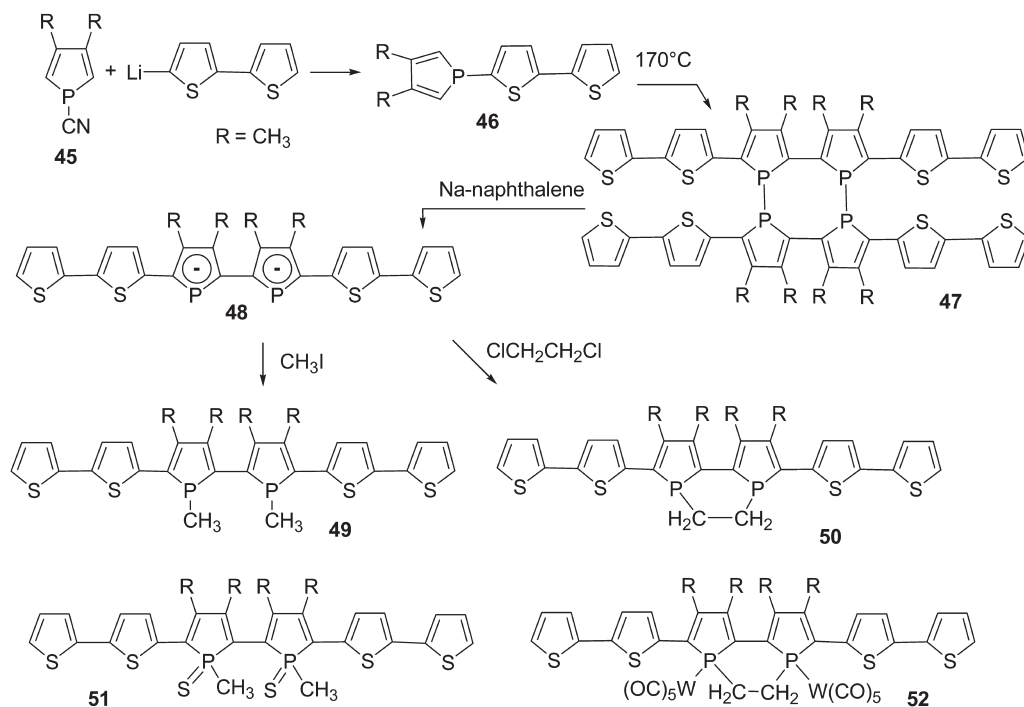
Hence it is clear that synthetic strategies are available for the synthesis of low molecular weight, well-defined mixed oligomers incorporating phosphole moieties. Comparison with related derivatives containing thiophene or pyrrole rings has, without a doubt, shown that the specific properties introduced by the presence of the P-heterocycle (e.g. low aromaticity, reactive heteroatom, σ - π hyperconjugation) afford these systems unique properties and considerable scope for further fine-tuning. Significantly, the mixed phosphole-based oligomers described in this section are more than simple model molecules since some of these compounds have already been used as active layers in OLED devices. These results prove that there are no inherent problems associated with the development of phosphole-based conjugated systems that possess optoelectronic functions. Furthermore, they clearly demonstrate that exploiting the reactivity of the P center of phosphole-derived oligomers could provide an exciting and powerful means of both optimizing and developing opto-electronic materials for the future.

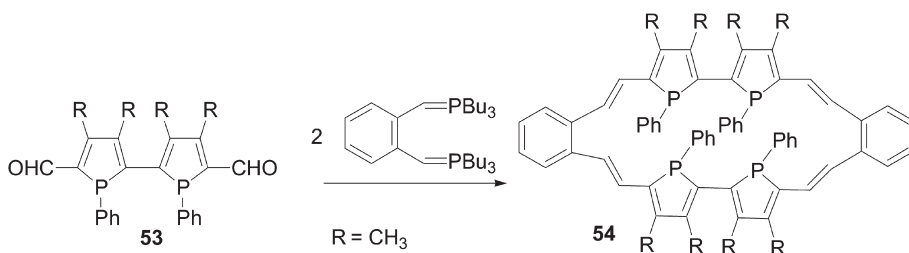
4.2.4

Mixed Oligomers Based on Biphospholes with other (Hetero)aromatics

Mathey and coworkers have prepared a series of dithienyl-capped biphospholes that are very attractive owing to the presence of electro-active termini and the potential diversity of structures that are available (e.g. linear, cyclic, P–C or P–P bonds). The synthetic strategies that afford these compounds are interesting, since they nicely illustrate some of the specific methods that can be used to prepare phosphole derivatives. For example, nucleophilic substitution at the P atom of phosphole **45** afforded the 1-bithienylphosphole **46** (Scheme 4.15) [43a]. Upon prolonged heating, this compound gave the cyclic tetramer **47** featuring biphosphole moieties, according to the mechanism depicted in Scheme 4.7. Reductive cleavage of the P–P bonds of **47** afforded the dianion **48**, which can subsequently be converted into the target dithienyl-capped biphospholes **49** and **50** (Scheme 4.15) [43a]. These derivatives are sensitive to oxidation and were isolated as adducts with sulfur or tungsten pentacarbonyl, derivatives **51** and **52**, respectively (Scheme 4.15).

An X-ray diffraction study of complex **52** showed that this mixed oligomer is not planar. The thiophene–thiophene, thiophene–phosphole and phosphole–phosphole twist angles are 6.35, 24.24 and 66.26°, respectively [43a]. Compound **51** un-





Scheme 4.16

dergoes two closely spaced successive one-electron reductions [43b]. Note that the reduced species $51^{\cdot-}$ and 51^- are relatively stable on the cyclic voltammetry (200 mV s⁻¹) time-scale, suggesting the existence of extended delocalization in these compounds [43b].

Cyclic oligomers based on phospholes are also available via Wittig reactions involving the 5,5'-bis(carboxaldehyde) **53** (Scheme 4.16) [44]. An X-ray diffraction study of **54** revealed that the four *P*-phenyl groups have an all-trans disposition and that this fully unsaturated macrocycle is distorted [44]. The cavity of the 24-membered heterocycle **54** is rather large, the diagonal distance between two P atoms reaching 6.1 Å.

4.2.5

Mixed Oligomers Based on Phospholes with Ethenyl or Ethynyl Units

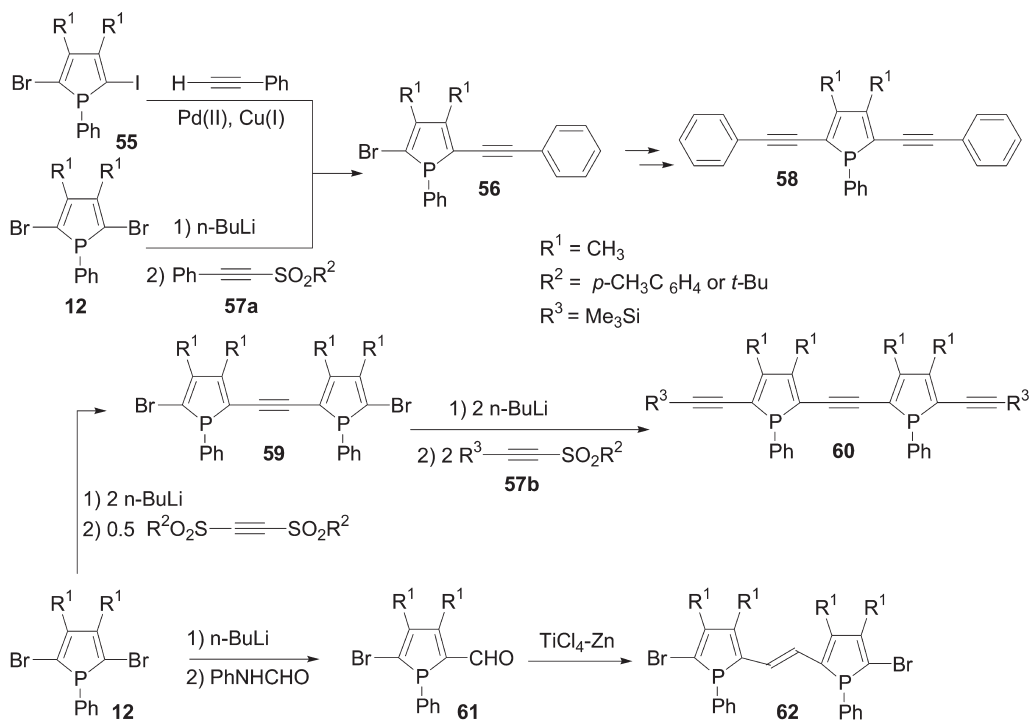
Oligomers and polymers consisting of alternating aromatic building blocks and either ethenyl or ethynyl units {e.g. PPV, oligo(thienylenevinylene)s [45a,b], poly(*p*-phenyleneethynylene)s [5k, 45c]} have found numerous applications in the fields of OLEDs, nonlinear optics, sensors, polarizers for liquid crystal displays, etc. Furthermore, the controlled synthesis of aromatic-ethynyl chains is driven by the need for molecular wires for the construction of a variety of nanoarchitectures [5e,i, 46]. Surprisingly, very few derivatives incorporating phosphole rings linked by a double or a triple bond have been reported to date. Once again, this is mainly due to the fact that the synthetic routes, especially metal-catalyzed C–C coupling reactions involving aromatic building blocks, are not efficient with phospholes. For example, neither 2-bromo-5-iodophosphole **55** nor its dibromo analog **12** undergo Stille-type couplings with 1-stannylalkynes, and the Sonogashira coupling of **55** with phenylacetylene afforded derivative **56** in only 10% yield (Scheme 4.17) [47a].

The key to the synthesis of such target ethynyl- and ethenylphosphole derivatives is the mono- and dilithiation of 2,5-dibromophosphole **12**. The intermediate 2-lithio-5-bromophosphole reacts with arylsulfonylacetylene **57a** (Scheme 4.17) to give rise to derivative **56**, which can be converted into α,α' -di(acetylenic)phosphole **58** according to the same general strategy as above. Although the yields of these reaction sequences are rather modest (typically around 30%), this syn-

thetic approach allows the stepwise preparation of derivative **60** from **12** by employing trimethylsilyl-protected alkynes **57b** (Scheme 4.17) [47a]. Disappointingly, the modest yields of this overall methodology preclude its use for the preparation of longer oligomers or polymers starting from **12** or **59**.

X-ray diffraction analysis of the model compound **58** revealed that the C–C linkages between the *P*-heterocycle and the C \equiv C moieties are rather short [1.423(3)–1.416(3) Å] [47a]. These data suggest that the endocyclic dienic π -system of the phosphole unit is efficiently conjugated with the two acetylenic substituents. The presence of an extended π -conjugated system for **58** is also supported by its orange color. The P atom adopts a pyramidal geometry and the P–C bond distances are typical for P–C single bonds [1.815(2)–1.821(2) Å]. Hence, as observed for 2,5-diheteroarylphospholes, the lone pair of the P atom does not interact with the π -system. Note that derivatives **59** and **60** are orange, which is again suggestive of the presence of an extended π -conjugated system [47a,b].

To date, only the simplest member of the oligo(phospholylenevinylidene) family, namely derivative **62** (Scheme 4.17), is known [47b]. This compound can be obtained in high yield, as the *E*-isomer, by a McMurry coupling with aldehyde **61** (Scheme 4.17) [47b]. Note that the use of Ti salts is compatible with the presence of σ^3 -P centers. No photophysical data for the orange mixed phosphole-ethenyl derivative **62** have been reported.



Scheme 4.17

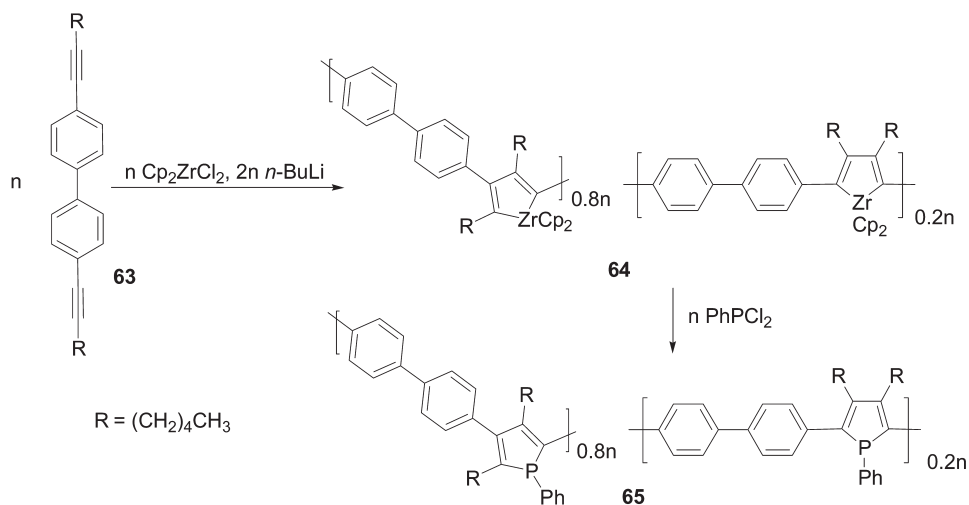
In conclusion, very few mixed oligomers based on phospholes combined with ethenyl or ethynyl moieties are known. Initial, but so far incomplete, data suggest that the compounds that have been studied are fully conjugated. This feature should motivate the synthesis of longer oligomers that are potentially accessible using bromo-capped building blocks. However, further progress is currently hampered by the low efficiency of coupling reactions involving phosphole rings.

4.2.6

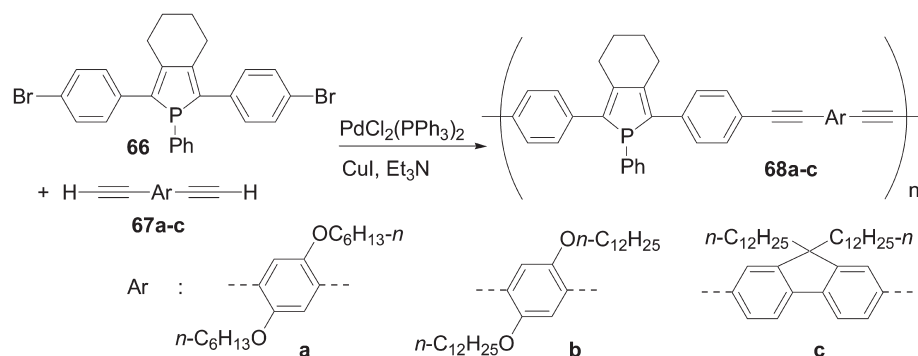
Polymers Incorporating Phospholes

To date, no homopolymers based on the phosphole motif are known. In contrast, a number of phosphole-containing copolymers have been reported. The first to be prepared was the biphenyl–phosphole derivative **65** obtained by Tilley and co-workers using the Fagan–Nugent methodology (Scheme 4.18) [48a]. Its synthesis involved the oxidative coupling of rigid diynes **63** with zirconocene, which proceeded in a non-regioselective way affording an 80:20 isomeric mixture of 2,4- and 2,5-connected metallacycles, respectively, in the polymer backbone of **64** (Scheme 4.18) [48a]. The reactive zirconacyclopentadiene moieties can subsequently be converted to the desired phospholes by adding dihalophosphine (Scheme 4.18) or to a range of other structures including dienes and benzene rings [48a–c].

Biphenyl–phosphole copolymer **65** is isolated as an air-stable and soluble powder exhibiting a rather high molecular weight ($M_w = 16\,000$; $M_n = 6200$) according to gel permeation chromatographic (GPC) analysis. Although multinuclear magnetic resonance spectroscopy and elemental analysis support the proposed structure, the presence of a small number of diene defects is very likely. Polymer **65**



Scheme 4.18



Scheme 4.19

exhibits a maximum absorption in its UV-Vis spectrum at 308 nm with a λ_{onset} value of 400 nm. These figures are consistent with a relatively high band gap, a feature probably due to a preponderance of cross-conjugated segments [48a]. Macromolecule **65** is photoluminescent; it emits in the bluish green region of the spectrum (470 nm) with a quantum yield reaching 9.2×10^{-2} .

A second type of π -conjugated polymer featuring a phosphole ring was obtained by Chujo et al. using the Heck-Sonogashira coupling of bromo-capped 2,5-(diphenyl)phosphole **66** [49a] with the diynes **67a-c** (Scheme 4.19) [49b]. Macromolecules **68a-c** are isolated in moderate to low yields as soluble powders, with low degrees of polymerization, ranging from 7 for **68c** to 15 for **68a**. The UV-Vis absorptions of **68a-c** are slightly red shifted in comparison with that of 2,5-diphenylphosphole, indicating the effective expansion of the π -conjugated system. The emission properties of these macromolecules depend on the nature of the comonomer. Green and blue emission are observed for **68a,b** and **68c**, respectively [49b]. However, the quantum yields in chloroform solution are modest (9–14%).

The most developed route to phosphole-containing polymers is the electropolymerization of thienyl-capped monomers, a process which involves the generation and coupling of radical cations [50]. Although this methodology is of great general interest for the preparation of electroactive materials based on thiophene or pyrrole monomers [5b,c, 50], it suffers from some significant drawbacks. The electrochemically-prepared polymers are often insoluble, preventing analysis by NMR or GPC. Furthermore, in addition to the desired α,α' -couplings that lead to fully conjugated polymers, α,β -couplings also take place [50]. The phosphole-containing monomers that have proved most successful in electropolymerization processes to date are depicted in Fig. 4.6. For example, the use of 2,5-(dithienyl)phosphole monomers **35–37** affords insoluble electroactive materials [15a, 31b]. The optimum polymerization potential E_{pol} , obtained by chronoamperometric investigations, depends on the nature of the P moiety (Table 4.3).

It is likely that the P atoms of the “as-synthesized” film obtained from the o^3,λ^3 -derivative **35** are protonated, at least partially, since the electropolymerization process generates protons [15a]. The polymers prepared with neutral phospholes

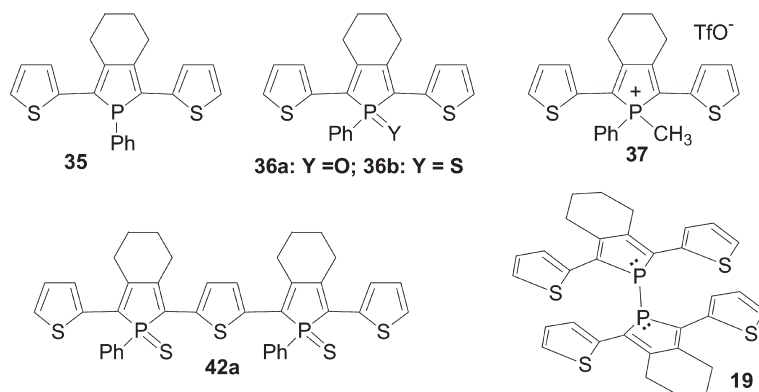


Fig. 4.6 Thienyl-capped monomers used in electropolymerization.

36a,b exhibited p- and n-doping characteristics with good reversibilities (>70%). Cationic poly-**37** also exhibits a reversible p-doping, but its electroactivity dramatically decreased upon reduction. It is noteworthy that these processes appeared at lower potentials than those of the corresponding monomers, suggesting that the electroactive materials possess much longer conjugation pathways and smaller band gaps than the monomers. This is confirmed by the fact that the values of λ_{onset} for the de-doped polymers were considerably red shifted compared with those observed for the corresponding monomers (Table 4.3) [15a,b]. A remarkable feature is that, as was observed for the P-containing monomers (Table 4.1), the electrochemical (doping range) and optical properties (λ_{max} , λ_{onset}) of these materials obtained by electropolymerization depend on the nature of the phosphorus moiety (Table 4.3). The electropolymerization of monomer **42a** (Fig. 4.6) also leads to an electro-active material presenting good reversible p-doping behavior [37]. The doping range (0.22–0.62 V) and λ_{max} of poly(**42a**) are comparable to those of poly(**36b**), as expected from their similar structures.

Table 4.3 Optimum electropolymerization potentials of monomers **35–37**, p-doping and n-doping potential ranges (V) and photophysical data for the corresponding dedoped polymers.

Monomer	$\lambda_{\text{max}}/\lambda_{\text{onset}}$ (nm)	$E_{\text{pol}}^{\text{[a]}}$ (V)	Polymer	p-Doping ^a	n-Doping ^a	λ_{max} (nm)	λ_{onset} (nm)
35	390/448	1.00	Poly- 35	0.50 → 0.85	–0.60 → –1.00	463–567	724
36a	434/500	1.10	Poly- 36a	0.25 → 0.60	–1.40 → –1.92	568	780
36b	432/496	1.15	Poly- 36b	0.30 → 0.65	–1.80 → –2.42	529	750
37	442/528	1.20	Poly- 37	0.40 → 0.70	–0.60	627	905

^[a] Potentials referred to the ferrocene/ferrocenium half-cell.

Monomer **19**, exhibiting σ - π conjugation (see Section 4.2.2), can also be electropolymerized by scanning in the -0.5 to 0.8 V potential range [25]. The cyclic voltammograms show the appearance and the regular growth of a new reversible wave with a threshold potential of about -0.35 V. The shape of the new anodic wave and the regular growth of the two initial anodic peaks along the recurrent sweeps indicate the conductivity of the deposited material (no shift to more positive potentials and no decrease in intensity). Poly-**19** can also be obtained readily by potentiostatic oxidation at $E_{\text{pol}} = 0.65$ V. The threshold oxidation potential of poly-**19** (-0.35 V) is the least anodic encountered in the series of thiophene-phosphole copolymers generated by electropolymerization (Table 4.3). The UV-Vis spectrum of poly-**19** exhibits a large band with an unresolved maximum at about 594 nm and a high value of λ_{onset} (73 nm) indicating a narrow optical HOMO-LUMO gap. This result shows that low-gap electroactive materials based on 1,1'-biphosphole units can be readily obtained by electropolymerization [25]. The low band gap is probably due to the existence of σ - π conjugation within these polymeric materials.

In conclusion, for the most part, polymers incorporating phosphole units are still rare. However, the work described above demonstrates that they are accessible via a number of diverse synthetic routes including organometallic coupling or electropolymerization processes. The general property-structure relationships established with well-defined small oligomers have been shown to extend to the corresponding polymeric materials.

4.2.7

Mixed Oligomers and Polymers Based on Dibenzophosphole or Dithienophosphole

Dibenzophospholes **A** and dithienophospholes **B** and **C** (Fig. 4.7) do not display the typical electronic properties and reactivity patterns of phospholes, since the dienic system is engaged in the delocalized benzene or thiophene sextet [7, 10a, 51]. In fact, these building blocks have to be regarded as nonflexible diaryl-phosphines or as *P*-bridged diphenyl or dithienyl moieties.

Dibenzophosphole **A** was in fact the first type of phosphole to be prepared [9], but it has only very recently been used as a building block for the preparation of π -conjugated systems. In this regard, polymer **70** is obtained with a high polydispersity ($M_n = 5 \times 10^2$; $M_w = 6.2 \times 10^3$) by Ni-catalyzed homo-coupling of derivative **69** (Scheme 4.20) [52]. The presence of σ^3 -P centers, which are potential donor sites for the Ni catalyst, does not prevent C-C bond formation. This macromolecule is photoluminescent in the solid state ($\lambda_{\text{em}} = 516$ nm), a property of potential interest for the development of OLEDs [52].

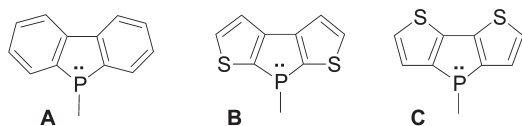
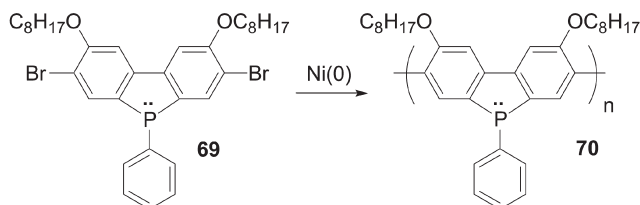
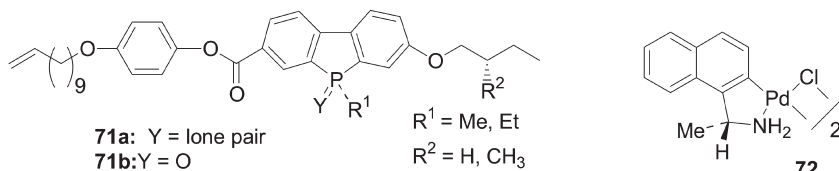


Fig. 4.7 Structures of dibenzophospholes **A** and dithienophospholes **B** and **C**.



Scheme 4.20



Scheme 4.21

Resolution of chiral σ^3 -benzophosphole **71a** (Scheme 4.21) was achieved by column chromatographic separation of the diastereoisomers obtained following its coordination to the chiral cyclometalated palladium(II) complex **72** [53]. This method nicely illustrates the advantages of having a P center present, which is able to coordinate to transition metals. The corresponding P-chiral dibenzophosphole oxide **71b** (Scheme 4.19) shows liquid crystalline behavior. Notably, the presence of a stereogenic P center is sufficient to generate a chiral cholesteric phase [53].

The dithienophosphole moiety **B** (Fig. 4.7) has been used to prepare cyclotriphosphazenes [54], but has not yet been investigated for the construction of π -conjugated systems. In contrast, dithieno[3,2-*b*:2',3'-*d*]phosphole **C** [55] has recently been considered for such purposes by Baumgartner et al. This building block is structurally related to heteroatom-bridged bithienyl moieties (Fig. 4.8), which exhibit interesting properties such as reduced HOMO–LUMO band gaps and hole-transporting capability [56].

The dithienophospholes **74** are obtained in good yields by lithiation of dibromobithiophenes **73**, followed by addition of dihalo(aryl)phosphines (Scheme 4.22) [57]. The Lewis basicity of the P center of **74** enables a broad range of facile chemical modifications to be undertaken, as exemplified with the synthesis of derivatives **75–77** (Scheme 4.22) [57].

Analysis of the bond lengths of compounds **75a,b** and the square-planar complex **77** in the solid state reveals a high degree of π -conjugation of the fused sys-

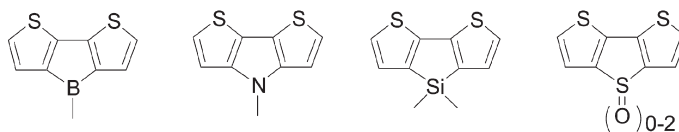
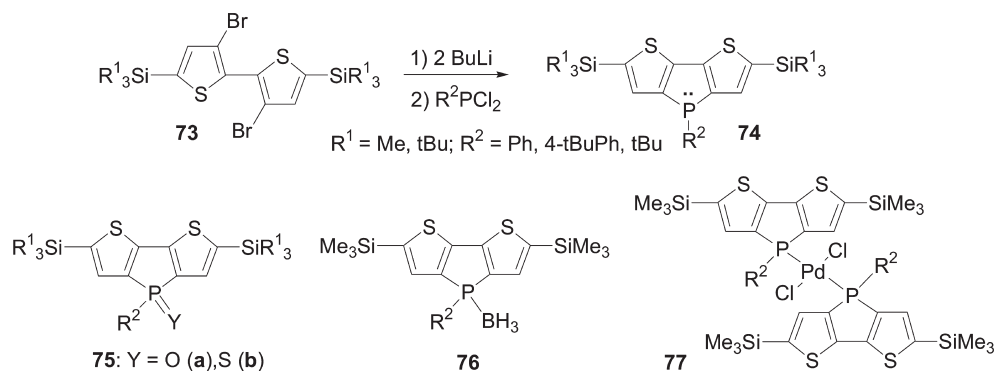


Fig. 4.8 Heteroatom-bridged bithienyl moieties. nAQ7n



Scheme 4.22

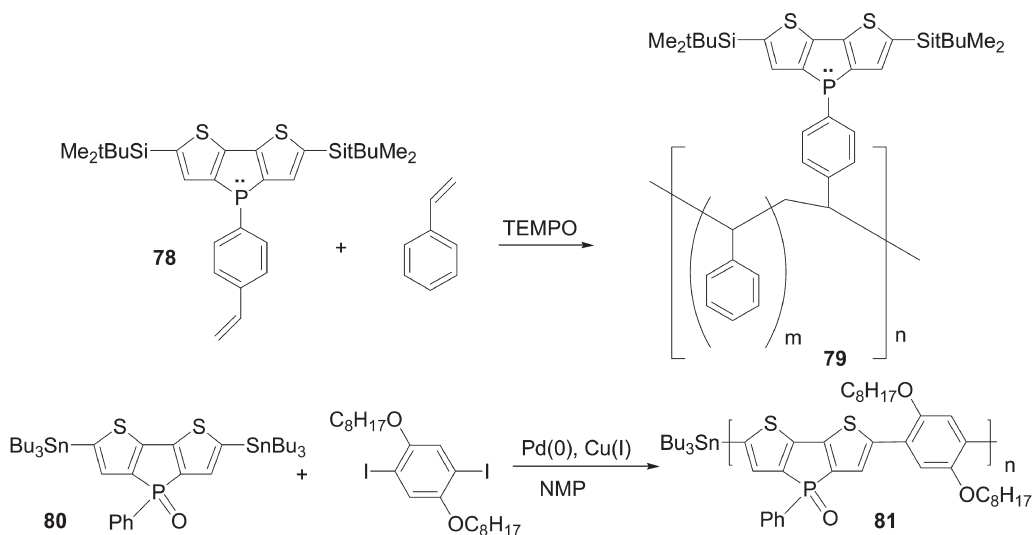
tem and the involvement of the acceptor silicon substituents in this delocalization [57]. These conclusions were confirmed by theoretical calculations [57c]. Derivatives **74** show absorption maxima due to π - π^* transitions in the UV region (Table 4.4). These data reveal, as expected for bridged dithienyl derivatives, rather high HOMO–LUMO separations. Chemical modification of the P center, leading to the formation of derivatives **75–77** (Scheme 4.22), induced a bathochromic shift in the value of λ_{max} , the most red-shifted value being that recorded for Pd complex **77** (384 nm) (Table 4.4) [57]. Note that modifying the substituents at the Si and P centers offers another tool for the further tuning of the values of λ_{max} for these systems. All these compounds exhibit strong blue photoluminescence with high quantum yields (Table 4.4). These PL quantum yields are far superior to those of 2,5-dithienylphospholes (Table 4.1), a feature that is probably due to the rigid structure of the dithienophospholes **74–77**.

Dithienophosphole units have been incorporated into polymers as either (i) side-chains or (ii) building block constituents of the extended polymer backbone itself. Polymers of the first type have been prepared by exploiting the ease with which a polymerizable styryl substituent may be introduced at the P atom of

Table 4.4 Physical properties of dithienophospholes **74** and derivatives **75–77**.

Compound	$\lambda_{\text{max}}^{[a]}$ (nm)	Log ϵ	$\lambda_{\text{em}}^{[a]}$ (nm)	ϕ_{f}
74 ($\text{R}^1 = \text{CH}_3$; $\text{R}^2 = \text{Ph}$)	344	4.26	422	0.604
75a ($\text{R}^1 = \text{CH}_3$; $\text{R}^2 = \text{Ph}$)	374	4.09	460	0.556
75b ($\text{R}^1 = \text{CH}_3$; $\text{R}^2 = \text{Ph}$)	374	4.00	460	0.556
76	355	4.10	432	0.545
77	384	4.03	470	0.614

^[a] In CH_2Cl_2 .



Scheme 4.23

dithienophospholes. Thus, the styryl derivative **78** was heated at 110°C in the presence of styrene (ca. 1:30 ratio) and a catalytic amount of 2,2,6,6-tetramethylpiperidinyl-1-oxy (TEMPO) (Scheme 4.23) [57b]. This reaction gave polymer **79**, which was subsequently characterized and shown to have a high molecular weight ($M_m = 147\,650\text{ g mol}^{-1}$) and a polydispersity of 2.46. The glass transition and decomposition temperatures of this material are 114.2 and 482.2°C , respectively. Multinuclear magnetic resonance spectroscopy revealed that the polymer had the desired dithienophosphole:styrene ratio of 1:30. This material exhibits a blue fluorescence, its λ_{max} (352 nm) and λ_{em} (424 nm) values match those observed for the monomer **78** (Scheme 4.23). The P atoms can be oxidized with hydrogen peroxide, but surprisingly, the photophysical properties of the polymer are not affected by this chemical modification at phosphorus [57b].

The second strategy for the formation of polymers that incorporate the dithienophosphole fragment utilizes a Stille coupling involving tributyltin-capped oxodithienophosphole **80** in *N*-methylpyrrolidinone (Scheme 4.23) [57c]. The resulting polymer **81** has a low solubility in THF, preventing its analysis by GPC. The values of λ_{max} (502 nm) and λ_{em} (555 nm) for **81** are significantly red shifted compared with those of the corresponding monomer **80** (λ_{max} 379 nm; λ_{em} 463 nm).

It is clearly evident that the various series of conjugated polymeric systems based on dithienophospholes that have been prepared are promising candidates for optoelectronic applications since their optical properties can be easily varied in a variety of different ways (chemical modifications of the P center, variation of the Si and P substituents, etc.). Furthermore, their potential scope in a range of applications is broadened by the possibility of incorporating these conju-

gated derivatives into polymeric systems either as constituents of the main polymer backbone or as side-chains. Thus, dithienophospholes can potentially be utilized both in 'small molecule' and 'polymeric' approaches for the fabrication of OLEDs.

4.3

Phosphine-containing π -Conjugated Systems

Incorporating heteroatoms bearing lone pairs (Fig. 4.9) into π -conjugated backbones is a powerful means of tuning the electronic properties of polymers [58]. The heteroatom can participate in π -conjugation by virtue of its lone pair, in addition to being a site for chemical modification allowing for further structural and property diversification. This strategy has only recently been investigated with phosphorus. The derivatives presented in this section are subdivided according to the nature of the organic subunits (namely phenyl and ethynyl).

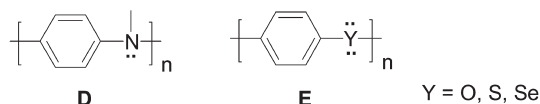
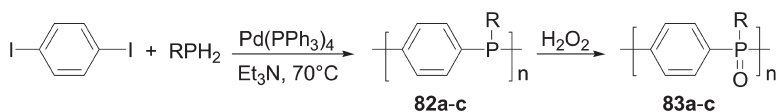


Fig. 4.9 Examples of polymers incorporating heteroatoms having a lone pair.

4.3.1

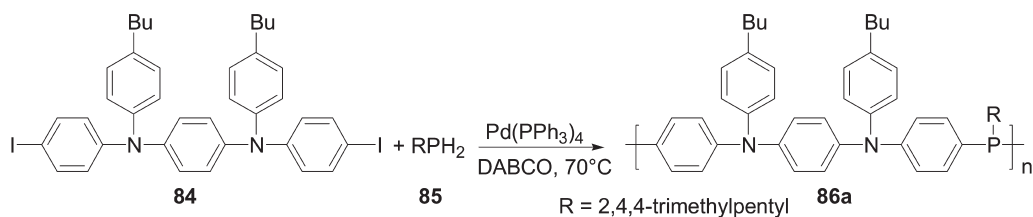
Polymers Based on *p*-Phenylenephosphine Units

Polyanilines **D** (Fig. 4.9) are amongst the oldest and best known photochromic materials. They are conveniently prepared by two different routes, namely polymerization of aqueous HCl solutions of anilines [58] or metal-mediated C–N bond formation from aryl halides or triflates with amines [58e,f]. Significantly, the first of these methods of polymer synthesis has not been reported with phosphorus-based monomers and it is likely that it will fail, owing to the profoundly different electronic properties of N and P centers. In contrast, the second route has been applied to the synthesis of poly(*p*-phenylenephosphine)s. Accordingly, polymers **82a–c** (Scheme 4.24) were obtained by palladium-catalyzed cross coupling of 1,4-diiodobenzene and primary aryl- and alkylphosphines [59a]. Owing to their good solubility, these materials were characterized by GPC and multinuclear magnetic resonance spectroscopy. They contain relatively short chains ($M_n = 1000\text{--}4000$) with narrow polydispersities (PDI = 1.3–1.5). The UV–Vis spectra of polymers **82a–c** show absorptions attributed to π – π transitions with values of λ_{max} ranging from 276 to 291 nm [59a]. The bathochromic shift observed on going from triphenylphosphine ($\lambda_{\text{max}} = 263$ nm) to 1,4-diphenylphosphinobenzene ($\lambda_{\text{max}} = 275$ nm) and then to **82b** ($\lambda_{\text{max}} = 291$ nm) suggests the presence of some extended π -delocalization involving the P lone pair in the latter material. However, the rather high band gap values are probably due to the fact that the



	<i>R</i>	<i>n</i>	λ_{max} (nm)
82a	CH ₂ CH(CH ₃) ₂	10	278, 415
82b	Ph	7	291, 434
82c	CH ₂ CH(CH ₃)CH ₂ C(CH ₃) ₃	14	276, 422

Scheme 4.24

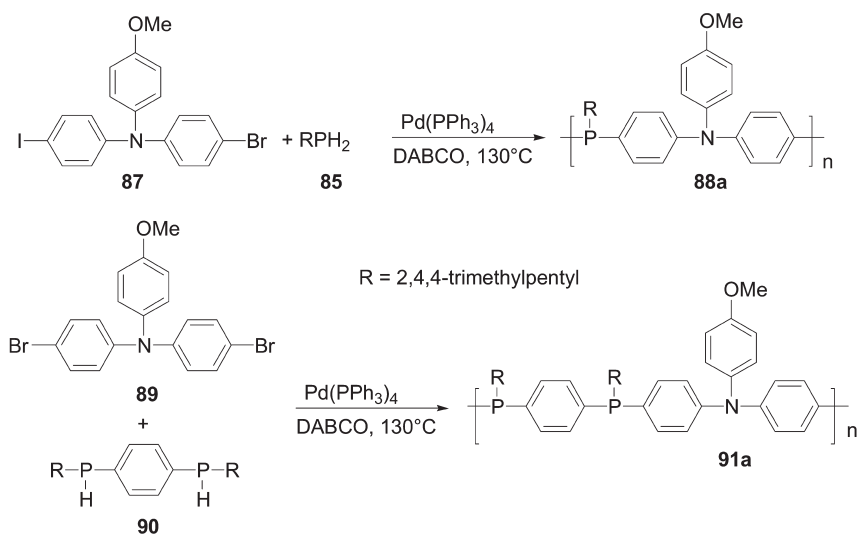


Scheme 4.25

P atoms retain a tetrahedral geometry that prevents efficient conjugation of the phosphorus lone pair with the aryl groups. Interestingly, oxidation with FeCl₃ in the absence of oxygen afforded paramagnetic polymers characterized by UV-Vis absorptions that are considerably red shifted in comparison with those of **82a-c**. The high value of λ_{onset} (ca. 800 nm) supports the presence of an extension to the conjugation path through the P atoms. Note that the P atoms of **82a-c** are still reactive. The oxidized materials **83a-c** exhibit a number of new absorption bands that are red-shifted compared with those of their precursors **82a-c** [59a].

Utilizing the same general palladium-catalyzed C-P bond-forming reaction, several different types of alternating poly(*p*-phenylenephosphine)-polyaniline polymers have been prepared. Derivative **84** reacted with primary phosphine **85** (1:1 ratio) to produce copolymer **86a** (Scheme 4.25) [59b]. Approximately half of the material is soluble in THF, with GPC analysis of this soluble fraction revealing it to be of low molecular weight ($M_n = 5000$) with a narrow polydispersity (PDI = 1.6). The remaining insoluble material is assumed to have the same structure, but much higher molecular weight.

The two-step polycondensation of the iodobromo derivative **87** with phosphine **85** afforded polymer **88a** (Scheme 4.26) [59b]. The THF-soluble part (about one-third of the material) consists of oligomers of low molecular weight ($M_w = 3000$, $n = 7$, PDI = 1.5). Derivative **91a**, possessing a P:N ratio of 2 and 16 repeat units ($M_w = 11\,000$, PDI = 1.9), was obtained via the same approach using bifunctional synthons **89** and **90** (Scheme 4.26). The higher molecular weight of **91a** vs. **88a** is simply due to its greater proportion of solubilizing 2,4,4-trimethylpentyl substituents. Note that it is very likely that the molecular weights, which are determined with reference to polystyrene standards, are underestimated [59b].



Scheme 4.26

The corresponding phosphine oxide copolymers **86b**, **88b** and **91b** (Fig. 4.10) have also been prepared in quantitative yields using hydrogen peroxide. They have been fully characterized by IR and NMR spectroscopic methods [59b]. Their molecular weights, as estimated by GPC, are about half of those observed for the corresponding σ^3 -derivatives, something that was assigned to a significant alteration in their conformation upon P oxidation.

Cyclic voltammetry revealed that the N-atoms of **86a**, **88a** and **91a** are oxidized at lower potentials than the trivalent P atoms. Comparison of these data with those observed with model compounds shows a very weak electronic delocalization via the P centers for copolymers **86a** and **91a**. In contrast, the low first oxidation potential observed for **88a** (Table 4.5) is assumed to result from an electronic communication between the N moieties through the connecting P centers [59b]. The equivalence of the oxidation potentials for the oxidized polymers (Table 4.5) suggests the presence of electronically isolated triarylamine fragments in these derivatives. Note that the involvement of the P lone pair in π -delocalization

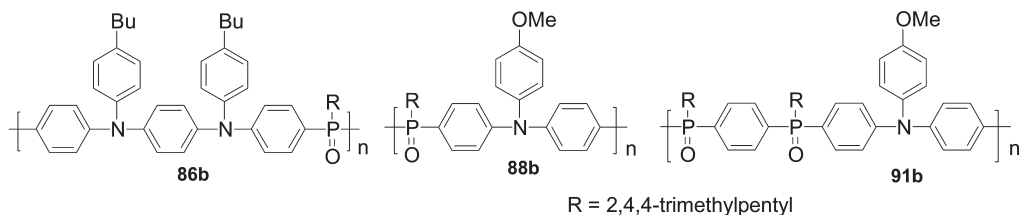
Fig. 4.10 Poly(*p*-phenylenephosphine oxide)-polyaniline polymers.

Table 4.5 Cyclic voltammetric data for copolymers **86a**, **88a** and **91a** and for the corresponding oxides **86b**, **88b** and **91b**^[a].

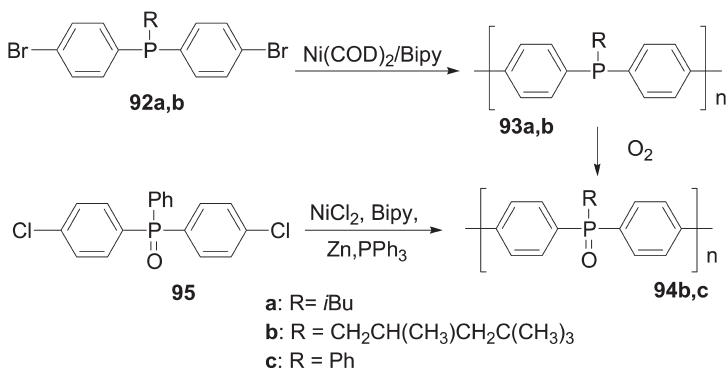
	86a	88a	91a	86b	88b	91b
E_{ox1} (V)	0.15	0.09	0.5	0.36	0.67	0.63
E_{ox2} (V)	0.45	0.83	0.79	0.73	–	–
E_{ox3} (V)	0.83	–	–	–	–	–

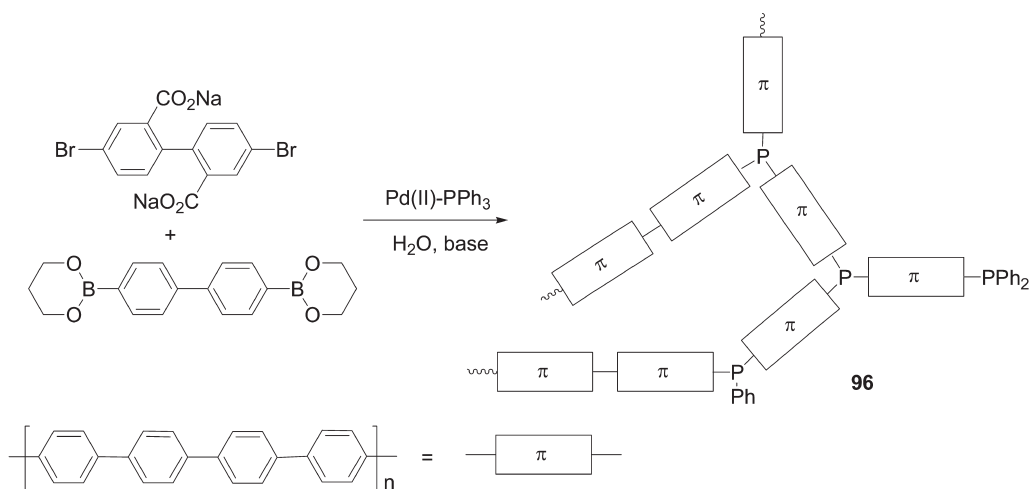
^[a] Ag/AgCl reference electrode in CH_2Cl_2 .

along the backbone in **88a** is supported by the large shift in oxidation potentials observed upon its conversion to **88b** (Table 4.5). UV-Vis-NIR studies of these compounds are consistent with these general conclusions [59b].

In summary, linear phosphorus-containing poly(*N*-arylanilines) can be readily obtained by palladium-catalyzed C–P bond formation. Their physical properties strongly support electronic delocalization through σ^3 -P centers along the polymer backbone, something that is switched off upon oxidation of the P atoms.

Biphenyl-phosphinidene polymers **93a,b** (Scheme 4.27) were prepared using Ni-catalyzed C–C bond-forming reactions with the bis(*p*-bromophenyl)phosphines **92a,b** [60a]. Disappointingly, this approach was found to be inappropriate for the formation of high molecular weight polymers. Thus, starting from **92a**, a dark-red insoluble solid was isolated, which was believed to be **93a**. Homo-coupling of phosphine **92b** bearing solubilizing groups afforded a low molecular weight ($M_n = 1000$), pale yellow material **93b** (Scheme 4.27). The color of **93b** is indicative of limited π -conjugation. This compound can be oxidized to afford **94b**. Note that the analogous *P*-Ph derivative **94c** can be obtained by Ni-catalyzed coupling of bis(*p*-chlorophenyl)phenylphosphine oxide **95** (Scheme 4.27) [60b]. The soluble material **94c** has a comparatively high molecular weight ($M_n = 15\,300$) together

**Scheme 4.27**



Scheme 4.28

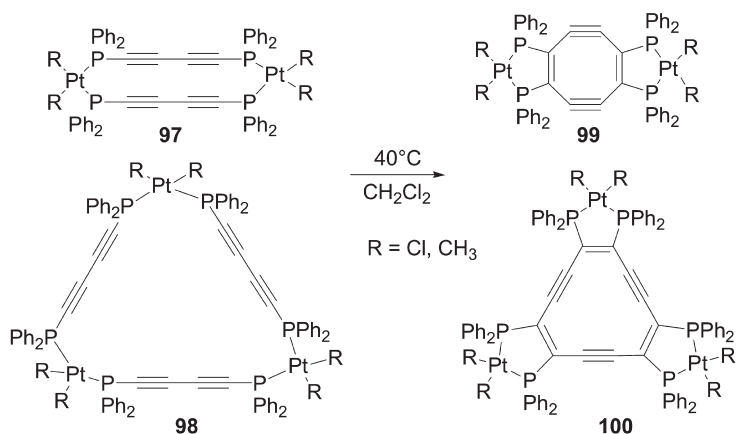
with a low molecular weight distribution (PDI = 1.6). It exhibits a high T_g (365 °C) with considerable thermal stability (< 5% weight loss at 550 °C). As expected, its very low absorption maximum ($\lambda_{\text{max}} \approx 280$ nm) discounts the presence of an extended π -conjugated system involving the P-moieties.

An example of a branched (*p*-phenylene) incorporating phosphorus moieties, **96** (Scheme 4.28), was obtained adventitiously during attempts to synthesize soluble linear (*p*-phenylenes) using Pd-catalyzed Suzuki couplings [61]. In fact, the formation of the branched polymer **96** arises from aryl–aryl interchange taking place with the intermediate $\text{Pd}(\text{Ar})(\text{I})(\text{PPh}_3)_2$ complexes [61b]. It should be noted that although the concentration of the phosphine ‘defects’ is very low, they have a significant impact on the properties (e.g. molecular weight, viscosity) of the polymers.

4.3.2

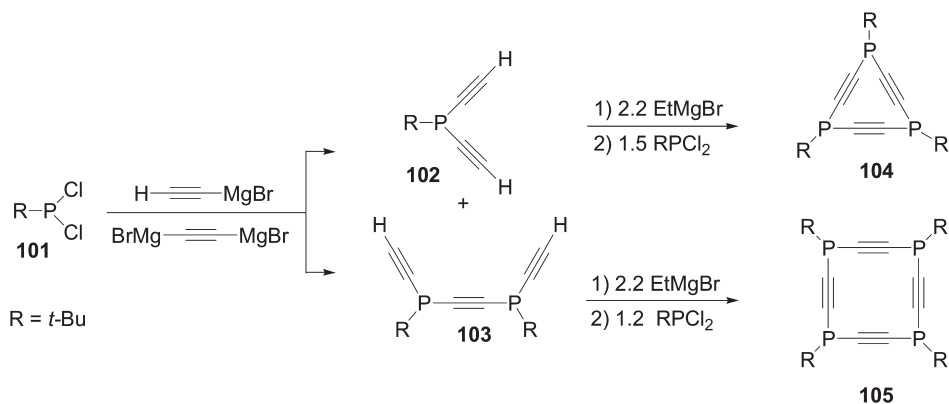
Oligomers Based on Phosphine–Ethyne Units

Phosphinoalkynes have been extensively used as rigid ligands in coordination chemistry [62]. In these cases, the role of the phosphino groups is simply to act as a two-electron donor towards transition metals, as exemplified by complexes **97** and **98** (Scheme 4.29) [62c]. When the ligands at Pt are chlorides, the phosphinobutadiyne rods undergo spontaneous [4 + 4] and [4 + 4 + 4] cycloadditions, leading to complexes **99** and **100** (Scheme 4.29) [62c]. These examples nicely illustrate how phosphinoalkynes can be used to build conjugated coordination oligomers or polymers. However, since the lone pair of the P atoms is clearly not involved in the conjugation, this type of derivative is not covered by this review.

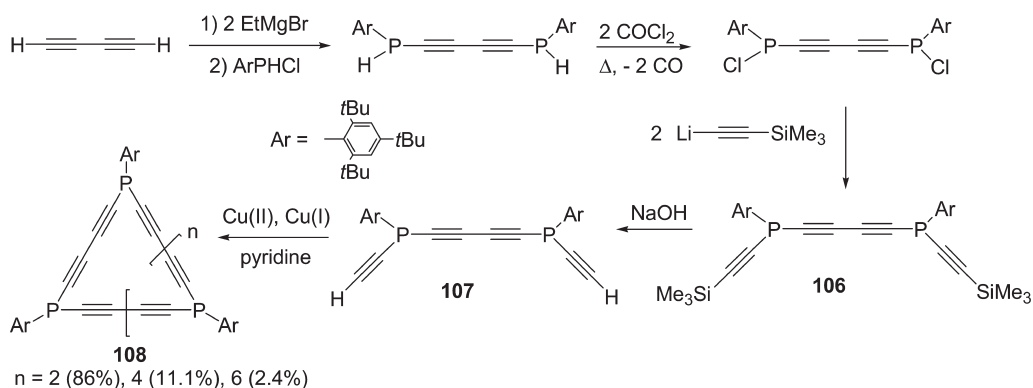


Scheme 4.29

Conjugated derivatives possessing phosphine–ethynyl units have mostly been prepared as building blocks for the synthesis of phosphaphericyclines and polyphosphacyclopolyynes. The routes used to prepare these compounds belong to the classical synthetic arsenal of transformations associated with the alkyne and halo-phosphine functions [63]. Thus, treatment of dihalophosphine **101** with an excess of ethynylmagnesium bromide gave rise to a mixture of compounds **102** and **103** isolated in 53 and 3% yield, respectively (Scheme 4.30) [64]. A double deprotonation of derivatives **102** and **103** followed by addition of 1.5 equiv. of P-electrophile **101** afforded triphospha[3]pericyclyne **104** and tetraphospha[4]pericyclyne **105** (Scheme 4.30). The UV–Vis spectra of the cyclic derivatives **104** and **105** showed strong absorption bands that extend out to nearly 300 nm, revealing that these P-heterocycles exhibit fairly strong cyclic electronic interactions [64].



Scheme 4.30



Scheme 4.31

A variety of linear ethynylphosphines, **106** and **107** (Scheme 4.31) and **109–112** (Scheme 4.32), have been prepared by Märkl et al. as synthons for the preparation of polyphosphacyclopolyynes **108** (Scheme 4.31) [65]. The ethynylphosphines **106** are obtained via a classical multi-step reaction sequence exploiting the electrophilic character of halophosphines (Scheme 4.31). The key steps involved in forming cyclic or linear oligomers are either Eglinton coupling of terminal alkyne moieties (Scheme 4.31) or a Cadiot–Chodkiewicz coupling involving bis-copper salts (Scheme 4.32). Derivatives **108** (Scheme 4.31) are obtained according to this random method as a mixture of di-, tri- and tetramers. Notably, these Cu-mediated C–C bond-coupling reactions are compatible with the presence of σ^3 -P moieties. One drawback of the presence of several P atoms is that the resulting compounds are obtained as a mixture of isomers.

An interaction between the phosphorus lone pairs and the ethynyl units is supported by several facts. First, derivative **106** (Scheme 4.31) possesses an unusually low inversion barrier (15.5 vs. 35 kcal mol⁻¹ for classical phosphines), indicating stabilization of the transient P-planar geometry. Second, the absorption maxima ($\lambda_{\text{max}} \approx 300$ nm) recorded for the heterocycles **108** (Scheme 4.31) and linear oligomers **109–111** (Scheme 4.32) ($\lambda_{\text{max}} = 210–308$ nm) are consistent with a degree of extended π -conjugation. However, the insolubility of the higher molecular weight, yellow oligomer **112** precluded UV–Vis analysis [65].

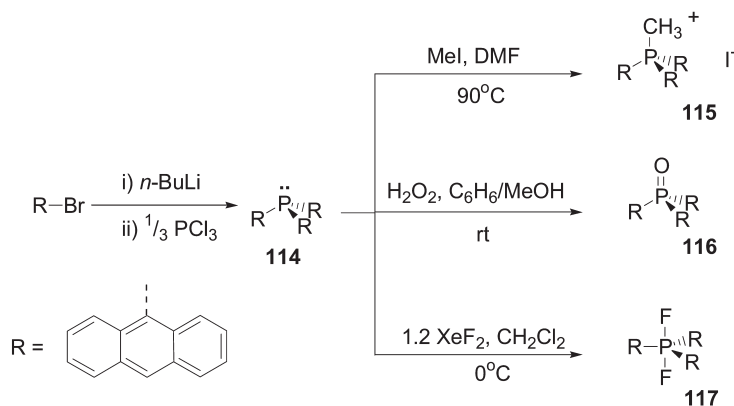
Thus, several routes to phosphine–ethynyl-based cyclic or linear oligomers are available and it is likely that these compounds possess extended conjugated systems involving the P lone pair. However, the development of this type of conjugated phosphorus system is hindered by the lack of efficient syntheses that allow for gram-scale preparations. This limitation is readily illustrated by the low-yielding preparation of dendron **113** (Scheme 4.33), something that precludes its use as a building block for higher generation dendrimers [66].

4.3.3

Mixed Derivatives Based on Arylphosphino Units

Chromophores based on aryl moieties can be easily grafted on to halophosphines via simple nucleophilic substitutions, as illustrated by the synthesis of **114** (Scheme 4.34). As a result, numerous phosphines bearing extended π -conjugated substituents have been prepared. The aim of this section is not to give a comprehensive account of all derivatives that have been synthesized, but rather to illustrate how phosphorus fragments can be used either to influence or to organize the π -conjugated systems, with special emphasis upon fluorescence and NLO properties.

The readily available σ^3 -phosphine **114** (Scheme 4.34) exhibits a broad absorption band at ~ 390 nm due to the π - π^* transitions associated with the anthracene moieties, together with a band at 437 nm, probably due to extended π -conjugation through the P lone pair [67a]. This compound was prepared in order to investigate the changes in physical properties induced by increasing coordination number at the heteroatom, as observed previously with triarylboranes and triarylsilanes [67b–d]. The σ^4 -derivatives **115** and **116** both possess tetrahedral geometry, whereas the σ^5 -phosphorane exhibits a trigonal-pyramidal geometry with the three anthracenyl moieties adopting an equatorial disposition. The UV-Vis spectra of derivatives **115**–**117** are blue shifted relative to that of **114** ($\Delta\lambda_{\text{onset}}$, ca. 40–80 nm). This shift can be ascribed to the inductive effects of the phosphorus moieties and/or to a through-space interaction between the anthracene substituents [67a]. Moreover, it has been established that the fluorescence properties are highly dependent on the coordination number of the central P atom. The σ^3 -phosphine **114** exhibits almost no fluorescence as a result of quenching by the P lone pair. The σ^4 -derivatives **115** and **116** show weak fluorescence with relatively large Stokes shifts, again presumably as a result of through-space interactions between the anthracene substituents. In sharp contrast, the pentacoordinate compound **117** shows an intense fluorescence; the quantum yield is ~ 30 – 100 times greater than

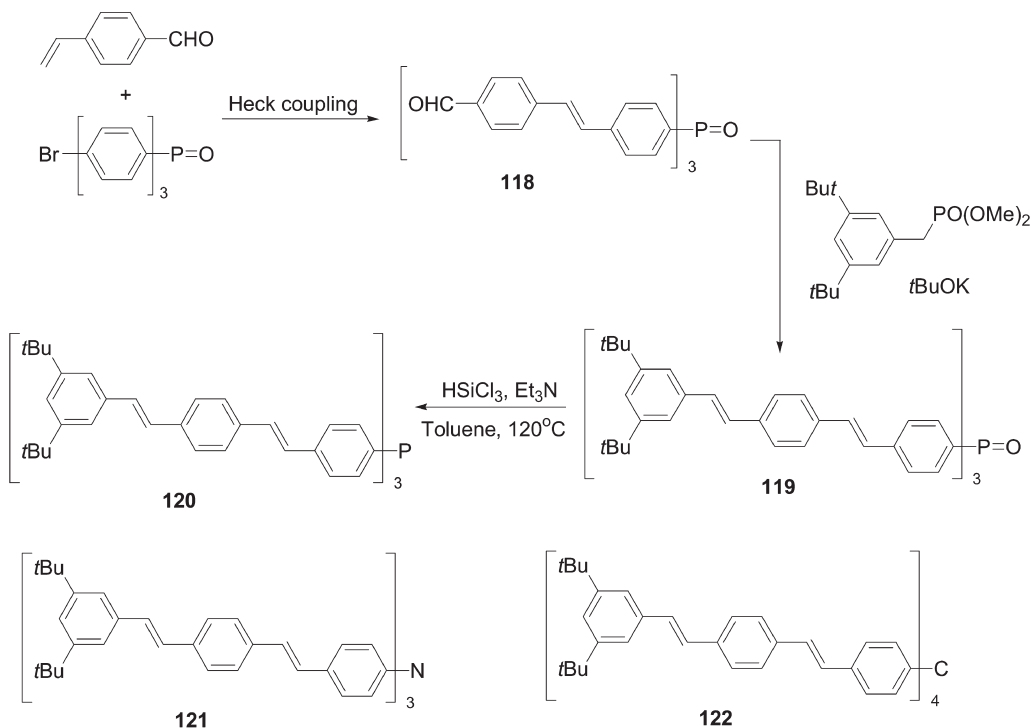


Scheme 4.34

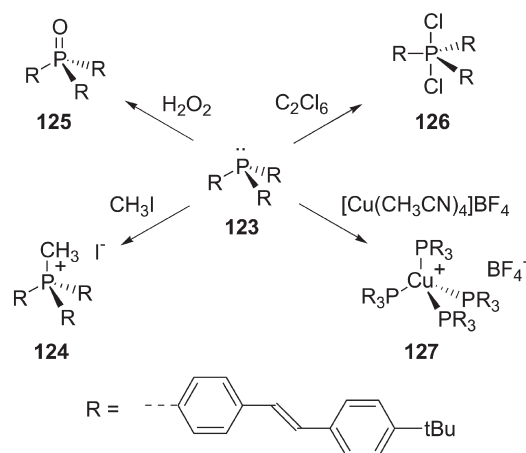
those of either **115** or **116**. Hence the fluorescence of the anthracene moiety is locked either by the presence of the P lone pair or by their pyramidal arrangement. These results give another clear example of property-control in conjugated systems through exploitation of phosphorus chemistry.

In order to investigate the optical excitations in multichromophore architectures, branched structures **120–122** (Scheme 4.35) bearing the same chromophore, but with different core units (C, N, P), have been investigated [68a]. The target P derivative **120** was prepared from a straightforward combination of a Heck coupling, to afford an intermediate functionalized stilbene phosphine oxide **118**, a Horner–Wittig reaction, yielding the phosphine oxide **119** and finally trichlorosilane reduction (Scheme 4.35).

It is assumed that the N-based system **121** is trigonal planar (in agreement with the planar structure of NPh_3 [68b]) and that the geometry of the central core P atom of **120** is more pyramidal than the C-derivative **122** [68a]. Examination of the UV–Vis spectral data reveals that the value of λ_{max} for the P-containing species **120** (376 nm) is red shifted relative to that for the C-cored compound **122** ($\lambda_{\text{max}} = 325$ nm), but blue shifted with respect to the N-based analog **121** ($\lambda_{\text{max}} = 430$ nm). This effect has been rationalized in terms of mesomeric effects. For the planar-cored compound **121**, an efficient overlap of the N lone pair with the adjacent carbon p-orbital gives rise to efficient conjugation with the chromophore substitu-



Scheme 4.35

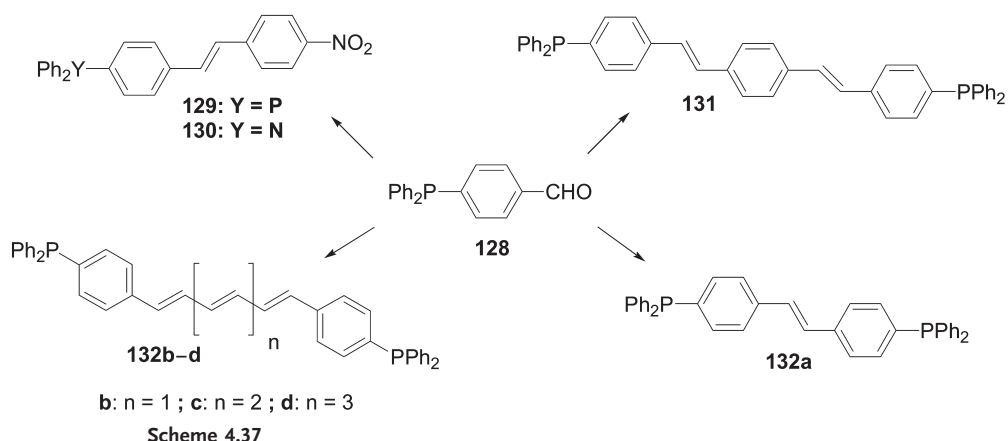


Scheme 4.36

ents, whereas for the larger pyramidal phosphorus of **120**, the overlap with the P lone pair will be significantly less efficient. Further studies to examine their fluorescence behavior revealed an incoherent hopping type of energy-transfer process, which dominates in the P derivative **120**. In contrast, a coherent mechanism is suggested for **121**.

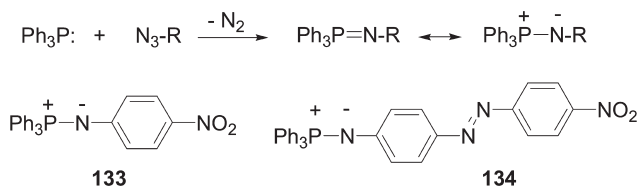
Together, these data show that both the structural arrangement of dipoles about the central single atom core and the extent of electronic delocalization through the heteroatom have a direct impact on energy transfer in branched conjugated structures [68a]. This nicely illustrates the effect of replacing an N atom by a P atom, a modification that induces a dramatic alteration in the compound's optical properties. These changes arise from the differences in the preferred geometries and electronic characteristics of the two heteroatoms. Furthermore, the presence of a reactive P atom potentially gives access to a whole series of derivatives with a variety of geometries, oxidation states and coordination numbers, as illustrated by the related tris(4-styrylphenyl)phosphine **123** (Scheme 4.36) [68c,d]. As observed for anthracene-substituted derivatives **114**–**117** (Scheme 4.34), the fluorescence behavior of the styrylphenyl phosphorus compounds **123**–**127** varies greatly depending on the coordination number and oxidation state of the P center. Once again, the presence of a P lone pair in **123** is responsible for fluorescence quenching; the hypervalent species **126** is the most efficient fluorophore. Note that an investigation of the photophysical behavior of a structurally related phosphine bearing *p*-(*N*-7-azaindolyl)phenyl substituents has shown that, at 77 K, this P compound displays both a fluorescence band ($\lambda_{\text{max}} = 372$ nm) and a phosphorescence band [$\lambda_{\text{max}} = 488$ nm, lifetime 38(6) ms] [68e].

Diphenylphosphino moieties have been investigated as auxiliary donor groups for the tailoring of potential second- and third-order NLO-phores, although their π -donating ability is clearly much lower than that of diarylamino units. The P-based systems are prepared using classical synthetic transformations (e.g. Wittig



reactions, McMurry couplings) starting from the aldehyde function of *p*-(diphenylphosphanyl)benzaldehyde **128** (Scheme 4.37) [69]. As expected, the value of λ_{max} for the P-based dipole **129** is blue shifted relative to that of its N analog **130** (Scheme 4.37). This variation could be of interest in terms of a trade-off between transparency and NLO activity, both of which are important parameters for the engineering of valuable second-order NLO-phores [70]. The same blue shift was also observed between the centrosymmetric diphenylphosphino-capped chromophores **131** and **132a-d** (Scheme 4.37) upon replacing N by P [68]. Note that these compounds have been designed to exhibit third-order NLO properties [68]. As expected, systematically increasing the number of conjugated C–C double bonds in the series of polyenes **132a-d** (Scheme 4.35) led to a pronounced red shift in the values of λ_{max} (**132b**, 341 nm; **132d**, 418 nm).

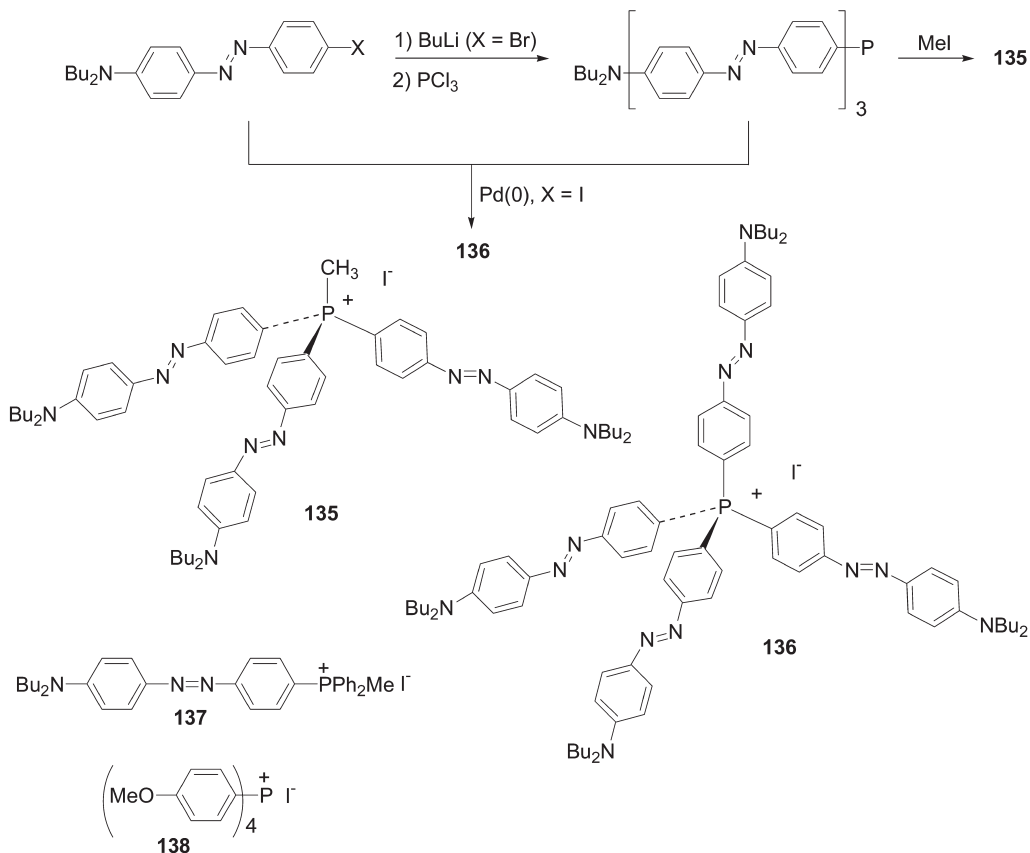
Iminophosphoranes (phosphazenes), compounds with the general structure R₃P=NR', are ylides possessing a highly polarized P=N bond [71]. With a view to optimizing push-pull NLO materials, they have been investigated as a new class of electron donors. Derivatives **133** and **134** (Scheme 4.38) are easily prepared by the so-called Staudinger reaction, which involves treating a tertiary phosphine with an organic azide (Scheme 4.38) [72]. The $\mu\beta$ product values of the resulting iminophosphoranes **133** and **134** are 310×10^{-48} and 1100×10^{-48} esu, respectively. These values are superior to that for *p*-nitroaniline (118×10^{-48}



esu), as expected from the significant donor ability of the iminophosphorane moiety, but are still modest compared with other efficient NLO-phores [70].

The search for efficient NLO-phores includes also the design of octupolar derivatives [40, 70a]. The advantages associated with this alternative class of NLO-phore include an improved nonlinearity–transparency trade-off and more facile noncentrosymmetric arrangement in the solid state due to the absence of dipolar moments. To this end, the 3-D chromophores **135** and **136** with C_3 and D_2 (approximate T) symmetry, respectively (Scheme 4.39), have been prepared according to classical synthetic routes [73a].

The UV–Vis data suggest that the subchromophores in **135** and **136** are near to being electronically independent. Derivative **135** has a small dipole moment and can be considered as an almost purely octupolar system, as is also the case for **136**. Compared with their tin analogs, the phosphorus derivatives **135** and **136** have higher β values owing to the more efficient acceptor nature of the phosphonium moiety [73a]. Furthermore, the NLO activity of the octupolar compound **135** is almost three times larger than that of the dipolar subchromophore **137**



Scheme 4.39

(Scheme 4.39), with almost no cost in terms of transparency. The related octupolar phosphonium salt **138** (Scheme 4.39) was investigated with the aim of obtaining NLO-active crystals that remain transparent across all, or nearly all, of the visible region [73b]. Structural analysis of **138** revealed a weakly distorted ionic structure of the NaCl type. The tetrahedral phosphonium ion retains an almost pure octahedral symmetry in the solid state. The crystal is transparent throughout the visible region and exhibits moderate NLO behavior [73]. Together these examples very clearly illustrate the potential of phosphorus derivatives for the engineering of octupolar derivatives.

Structurally related P-branched multichromophores have also been designed for potential application in materials for OLED fabrication or as sensors. Notably, the branched tris(diphenylaminostilbenyl)phosphine **139** (Fig. 4.11) has been successfully used as a hole-transporting material in OLEDs [74a]. Not surprisingly, the values of λ_{max} for **139**, in solution (300 and 392 nm) and as a thin film (302 and 389 nm), are both blue shifted compared with those of its N analog **140** (309 and 410 nm). Note that in this series, substitution of P for N results in improved thermal stability. OLEDs having an ITO/**139**/Alq₃/Mg:Ag/Ag composition exhibit an EL efficiency of 0.13 % for a voltage of 11.8 V at a constant drive current of 13 mA cm⁻² [74a]. This EL efficiency is higher than that obtained using the corresponding N derivative **140** (0.09 %), but rather low compared with devices utilizing NDP as the hole-transporting material.

Derivative **141** (Scheme 4.40) was designed as a fluorescent molecular sensor exploiting the presence of a triphenylphosphine oxide function, which is known to coordinate cations and the fluorescent phenylacetylene moieties [74b]. This compound is prepared in ca. 30 % yield according to the route depicted in Scheme 4.40. As observed with the structurally related styryl-substituted phosphine oxides **119** (Scheme 4.35), there is only an extremely weak (if any) interaction between the chromophores in the ground state for **141**. As expected, phosphine oxide **141** is strongly fluorescent with quantum yields varying from 0.71 to 0.89 % according to the nature of the solvent.

Hence it is clear that conjugated derivatives based on arylphosphino units are relatively easily prepared using either nucleophilic substitution with halophosphines or chemical modification of the phenyl moieties of arylphosphines. In most cases, the lone pair of the P atoms is only marginally involved in π -conjugation with the aryl substituents. Thus, the role of the P centers is mainly to organize the chromophores in a predictable way and to generate structural diversity via chemical modification at phosphorus. This general strategy has also been illustrated by the preparation of electrochemically generated polythiophenes

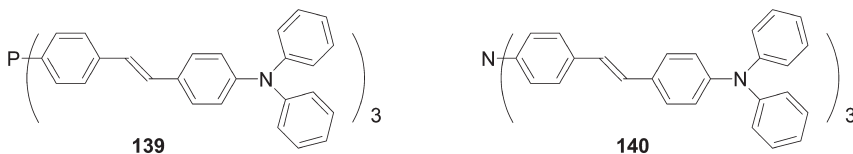
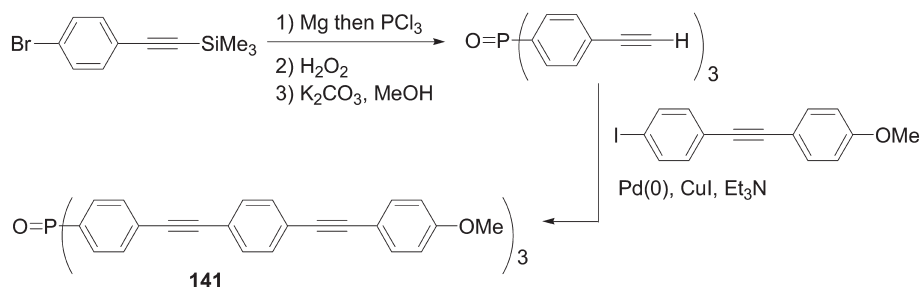
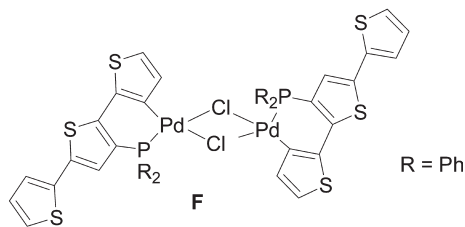


Fig. 4.11 Tris(diphenylaminostilbenyl)-phosphine and -amine.



Scheme 4.40

that incorporate metal functionalities, with a view to modifying the electrochemical properties of the resulting macromolecules. A diphenylphosphino-functionalized terthiophene reacts with a source of palladium(II) to afford the cyclometalated complex **F** (Fig. 4.12). Subsequent electropolymerization gives palladium-containing polythiophene whose conductance and electronic properties are modified via inductive effects from the metal relative to those of the parent polythiophene [75].

Fig. 4.12 Structure of cyclometallated complex **F**.

4.4

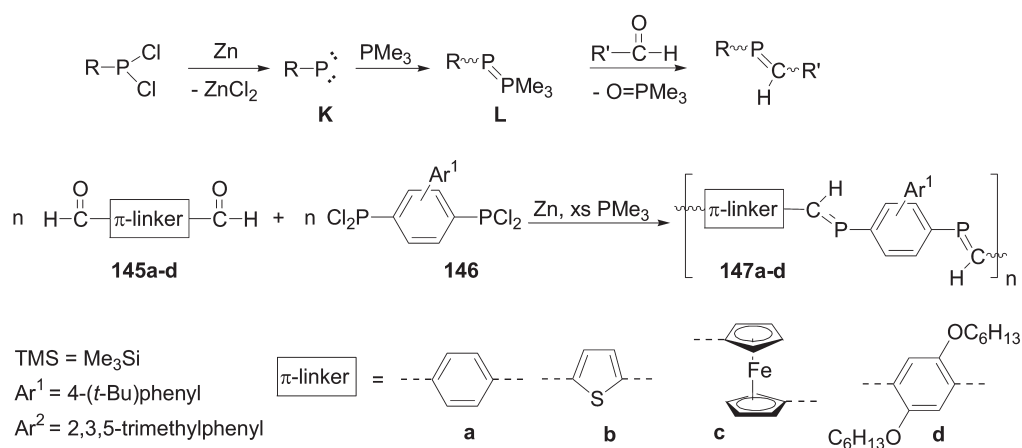
Phosphaalkene- and Diphosphene-containing π -Conjugated Systems

The properties and reactivity of low-coordinate carbon and phosphorus species are very similar in many regards [7]. Many of the parallels that exist between C=C and P=C bonds are due to the similar electronegativities of the two elements (C, 2.5; P, 2.2) and to the fact that, in marked contrast to imines, the HOMO of phosphaethylene is the π -bond and not the heteroatom lone pair [7a]. As a consequence, the P=C unit is almost apolar and its conjugative properties are comparable to those of the C=C bond [7, 76]. The concept that low-coordinate phosphorus behaves more like its diagonal relative carbon than its vertical congener nitrogen is now well accepted and has proved to be a fruitful tool for the design and synthesis of a raft of different compounds [7b]. Using this diagonal analogy, the simplest π -conjugated system incorporating phosphorus that can be envisaged would be poly(phosphaalkyne) **H** (Fig. 4.13), the P-containing analog of polyace-

of *Z*- and *E*-isomers, with the degree of polymerization varying from 5 to 21. Remarkably, thermogravimetric analysis revealed that this polymer is stable up to 190 °C under an atmosphere of dry helium [78b].

The family of P=C-containing polymers was considerably broadened following the introduction of a highly efficient synthetic strategy based on intermediate “phospha-Wittig” reagents **L** [79], obtained by reacting the transient phosphinidene **K** with PMe_3 (Scheme 4.42). Polymers **147a–d** featuring different π -linkers were readily obtained by reacting dialdehydes **145a–d** with the bulky bis(dichlorophosphine) **146** (Scheme 4.42) [80a]. Derivatives **147a–c** are insoluble materials, whereas macromolecule **147d** is soluble and has been shown to contain an average of 12 phosphaalkene moieties per chain ($n = 6$) in an *E*-configuration. Remarkably, although **147d** decomposes slowly in solution, it is stable under air for 1 week in the solid state [80a].

Derivatives **144** (Scheme 4.41) and **147d** (Scheme 4.42) exhibit broad absorption bands, with values of λ_{max} of 328–338 and 445 nm, respectively, that presumably result from π – π^* transitions. For comparison, model diphosphaalkenes **148** [78b] and **149** [80a] (Fig. 4.14) show absorption maxima at 314 and 445 nm, respectively. Hence the UV spectrum of polymers **144** is red shifted by only 20 nm compared with **148** whereas polymer **147d** and derivative **149** have identical values of λ_{max} . However, note that the bands arising from the polymeric derivatives extend into the visible region with values of the optical end absorption (λ_{onset} : **144**, ca. 400 nm; **147d**, ca. 540 nm), which are red shifted compared with those of the model compounds **148** and **149**. These data suggest that the P=C functions are effectively involved in the π -conjugation, but reveal rather limited effective conjugation path lengths for derivatives **144** and **147d**. This feature could be due to rotational disorder caused by the presence of the bulky aryl units, an idea supported by the X-ray diffraction analyses of **152** (Fig. 4.15), which reveals HCP–phenyl dihedral angles of 71 and 22° [80b]. The dramatic impact of such sterically induced noncoplanarity is also clearly reflected by the different values of λ_{max} obtained for **152** and



Scheme 4.42

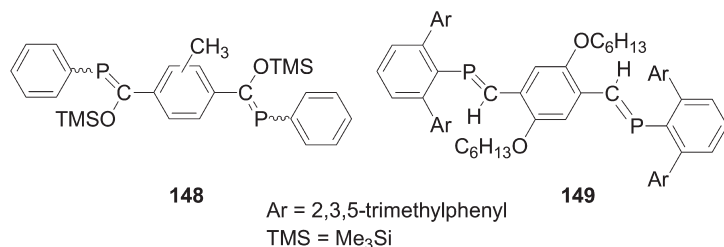


Fig. 4.14 Structures of model diphosphaalkenes.

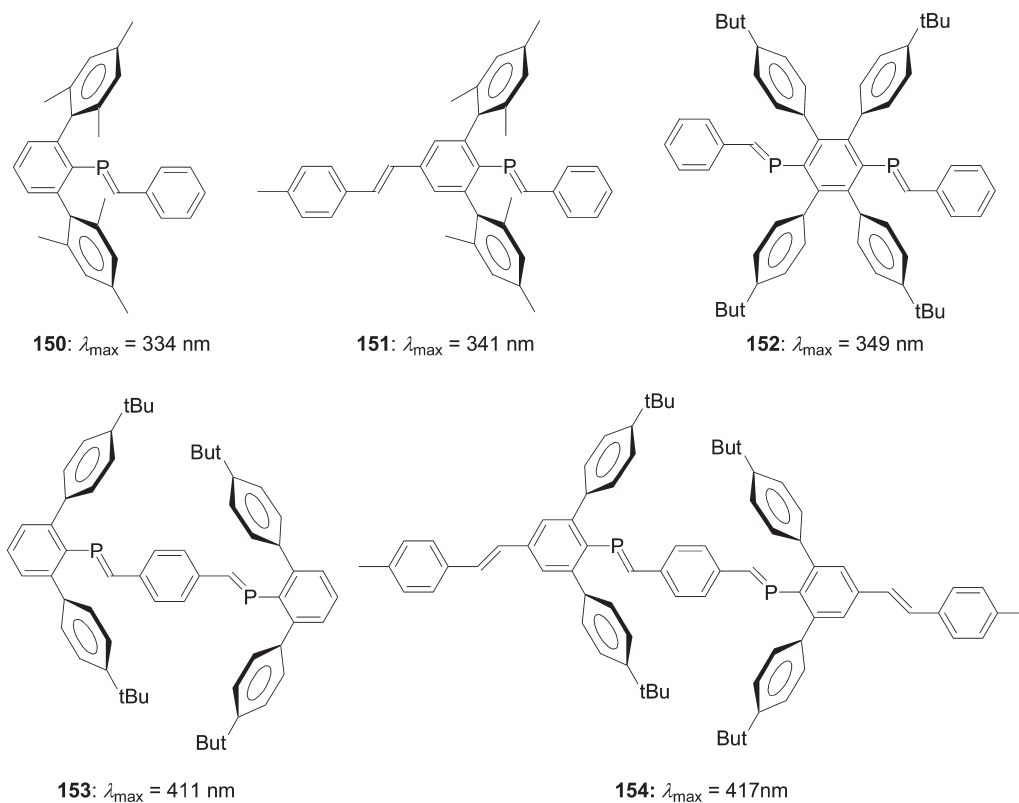
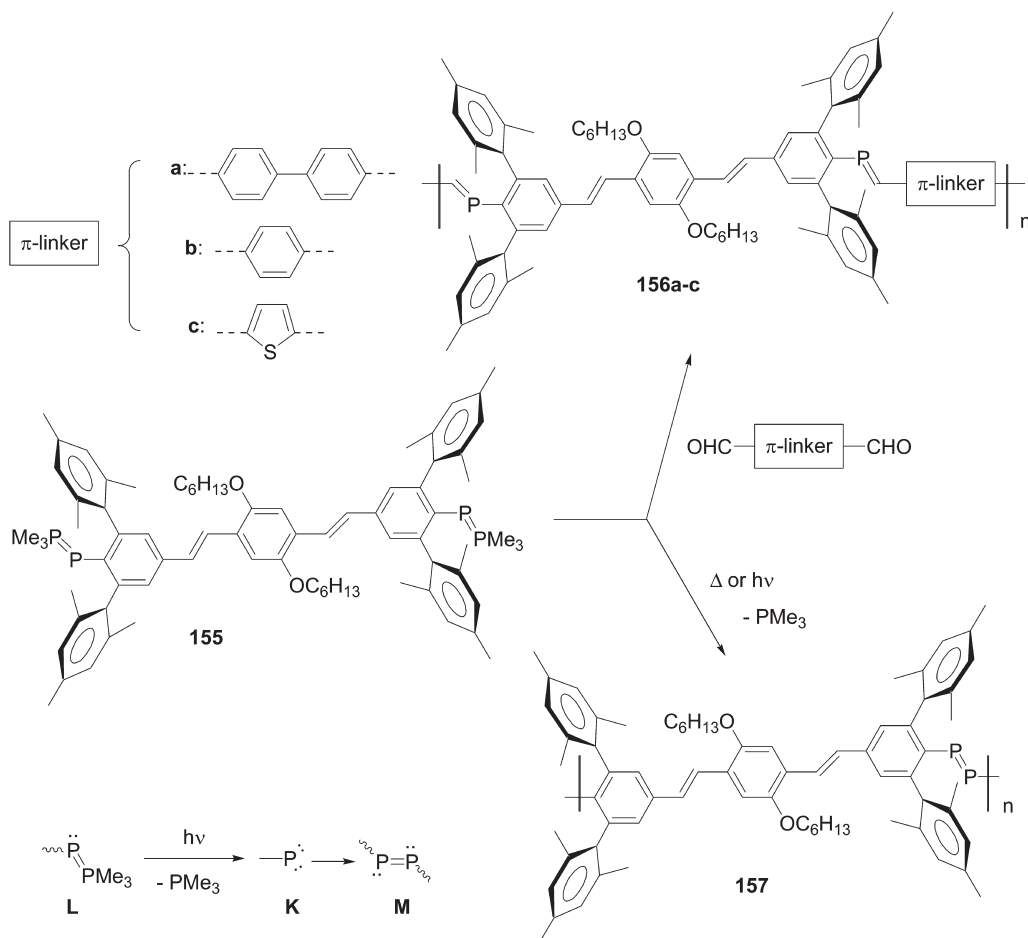


Fig. 4.15 Conjugated systems incorporating phosphaalkene moieties.

153 ($\Delta\lambda_{\max}$ = 57 nm, Fig. 4.15), which possess the same geometric conjugation path length [80c]. Note that the red shift observed upon comparing systems with a similar positioning of the sterically demanding units and increasing conjugation path length (150/151/152; 153/154) strongly supports the involvement of phosphaalkene moieties within the conjugated chain. Notably, polymer 147d showed fluorescence with a broad emission centered around 530 nm [80a]. How-



Scheme 4.43

ever, the fluorescence intensity is weak compared with those from its corresponding all-carbon analogs.

The formation of conjugated systems featuring P=P units is very challenging since this very reactive moiety needs significant steric protection in order to engender stability [76b, 81]. For such purposes, the sterically demanding 2,5-dimethylphenyl substituent was employed by Smith and Protasiewicz [80d]. This bulky fragment was used initially to stabilize P=C units in polymers **156** that were prepared in 76–85 % yields via a phospho-Wittig reaction (Scheme 4.43). The phosphorane alkenes adopt an *E*-configuration. The degree of polymerization is rather modest ($M_n = 5000$ – 7300) and the polydispersities vary from 1.9 to 2.3 [80d]. These derivatives are reasonably thermally stable in the absence of air or water. For example, polymers **156a** and **b** are unaffected by heating at 140°C for 6 h under an inert atmosphere.

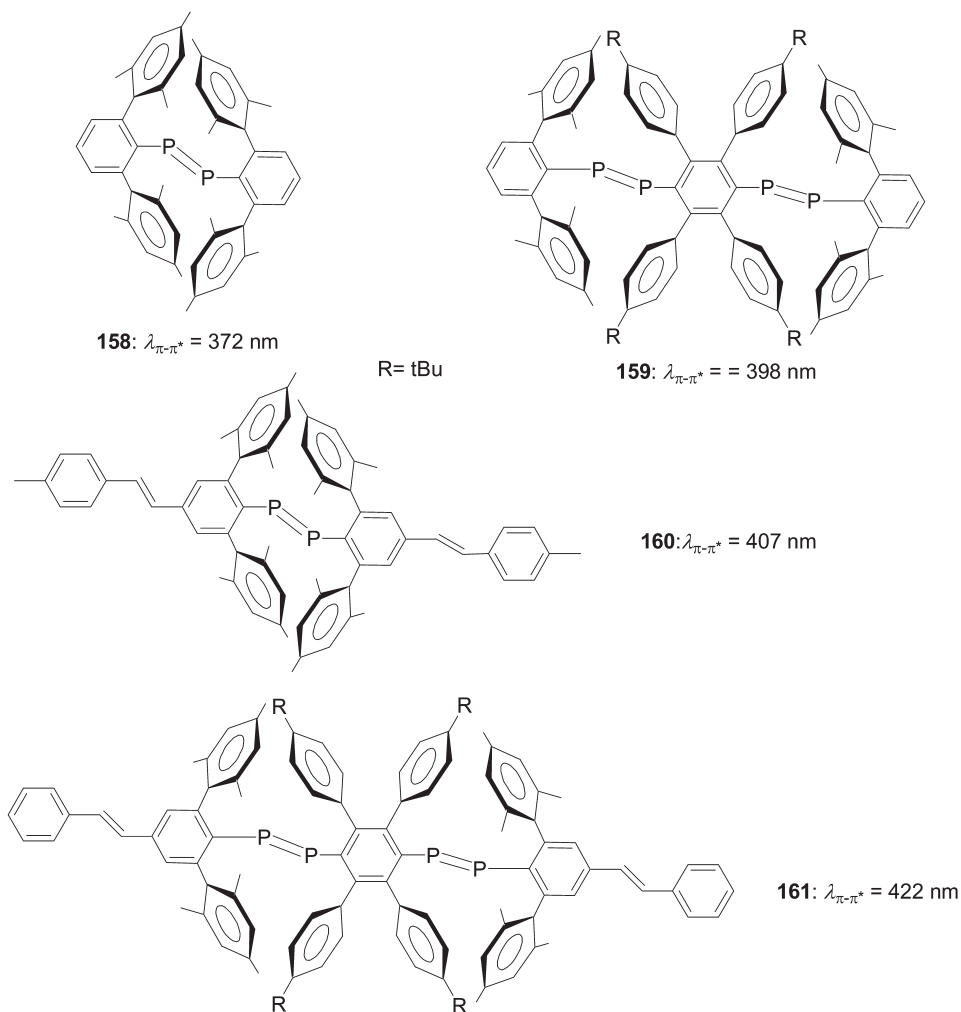


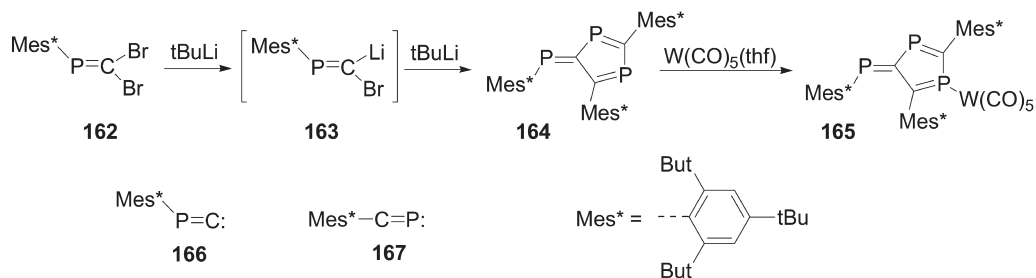
Fig. 4.16 Conjugated systems incorporating diphosphene moieties.

Subsequently, following the successful isolation of stable phosphalkene-containing polymers **156**, the use of the same substituent for the preparation of a related polymer featuring P=P moieties was attempted. It is known that diphosphenes **M** can be prepared by dimerization of transient phosphinidenes **J** generated by photolysis of phospho-Wittig reagents **L** (Scheme 4.43) [80e]. Photolysis at room temperature or thermolysis (neat, 250 °C, 2 min) of bifunctional compound **155** does indeed result in the formation of polymer **157** in near quantitative yield (Scheme 4.43) [80d]. This soluble material was characterized by NMR spectroscopy and GPC analysis, which revealed a rather low molecular weight ($M_n = 5900$). The UV-Vis spectrum of **157** shows a $\pi-\pi^*$ transition (435 nm) accompa-

nied by an $n-\pi^*$ transition that is red shifted (481 nm). The $\lambda_{\pi-\pi^*}$ value for **157** is in the range observed for **156a–c** (416–435 nm) and only slightly blue shifted compared with poly(phenylenevinylene-*alt*-2,5-dihexyloxyphenylenevinylene) ($\lambda_{\pi-\pi^*} = 459$ nm) [82]. These data indicate that diphosphene units support conjugation across extended systems. The validity of this assumption was enforced by the observed red shift within the series of compounds **158–161** of increasing chain length (Fig. 4.16) [80b]. Notably, in contrast to polymers **156a–c** featuring P=C units, the diphosphene-based derivative **157** is not fluorescent [80e].

Collectively, these studies show that oligomers incorporating phosphaalkene or diphosphene moieties are readily available by a variety of different routes and prove that the P=C and P=P units are capable of supporting conjugation across extended π -systems. Although structure–property relationships have still to be established, it is clear that macromolecules with higher degrees of polymerization and less sterically demanding substituents are exciting targets.

A last family of conjugated systems featuring P=C moieties that is worthy of note contains a fulvene structure. The reaction of dibromophosphaethene **162** with *tert*-butyllithium afforded the carbenoid **163**, which transformed into the deep-red 1,3,6-triphosphafulvene **164** (Scheme 4.44) [83a]. The latter compound can formally be regarded as a trimer of phosphanylidene carbene **166**, but the mechanism for its formation probably involves the generation of phosphalkyne **167** (Scheme 4.44). The results of an X-ray diffraction study of the tungsten pentacarbonyl complex **165** showed that the triphosphafulvene framework is planar, as expected [83a]. Derivative **164** undergoes a reversible one-electron reduction at -0.68 V versus Ag/AgCl [83b]. Note that related 1,4-diphosphafulvenes (Fig. 4.17) having different substitution patterns were described recently [83c–e].



Scheme 4.44

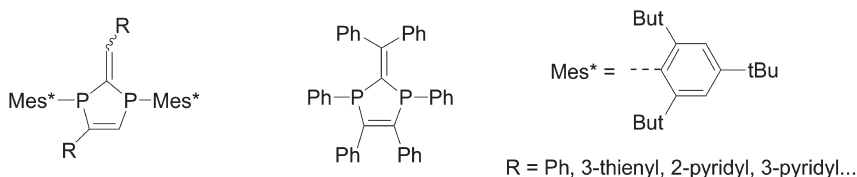


Fig. 4.17 Structures of 1,4-diphosphafulvenes.

4.5

Conclusion

The chemistry of π -conjugated systems incorporating P moieties has really only come to the fore following the pioneering work started in 1990 on phosphole-based oligomers and that on related phosphine–ethynyl co-oligomers. The last 5 years have seen a considerable expansion of the area with the synthesis of a plethora of novel P-based derivatives, together with the elucidation of their physical properties. Useful P-containing building blocks include heterocycles (e.g. phospholes), phosphino groups and low-valent phospho- and diphosphaalkenes. However, the chemistry of π -conjugated systems incorporating P units remains in its infancy, something that is nicely illustrated by the fact that the most recent review devoted to the synthesis and properties of conjugated molecular rods [5g] does not even mention organophosphorus building blocks!

Despite being a relatively young area of research, it has already been clearly established that organophosphorus derivatives offer specific advantages over their widely used sulfur and nitrogen analogs. Of particular interest is the possibility of chemically modifying P centers, something that provides a unique way to create structural diversity and to tune the physical properties of these phosphorus-based π -conjugated systems. This facet is of particular importance for the tailoring of organophosphorus materials for applications in optoelectronics. Moreover, the coordination ability of P centers towards transition metals offers manifold opportunities to build supramolecular architectures in which the π -systems can be organized in a defined manner. A great variety of synthetic routes have been used, but new strategies have to be developed in order to generate well-defined series of oligomers and polymers. Structure–property relationships have still to be established in order to exploit fully the potential of P moieties in the construction of conjugated frameworks.

A number of problems still remain that prevent the use of P-based π -conjugated systems from reaching real applications (e.g. thermal and chemical stability, solubility). However, the well-established and highly developed understanding of the chemistry of phosphorus-containing compounds, including both low-valent and heterocyclic species, will allow most of the remaining issues to be circumvented. Indeed, the possibility of using organophosphorus π -conjugated systems as materials for applications in the field of nonlinear optics, organic light-emitting diodes and conductive polymers has already been firmly demonstrated. Hence there is no inherent limitation associated with the use of conjugated phosphorus-containing materials for these important and appealing end uses. However, considering the richness and diversity of phosphorus chemistry, their true potential has not yet been fully exploited. It is very likely that new developments will occur in these areas in the near future, which will take full advantage of the specific properties of organophosphorus derivatives.

4.6

Selected Experimental Procedures

Synthesis of tetramer (**22**) (Scheme 4.7) [28a,c]

3,4-Dimethyl-1-phenylphosphole **4** (2.26 g, 12 mmol) and *N,N'*-dimethyl-4-bromoaniline (1.8 mmol) were heated in a sealed glass tube at 180 °C for 18 h. The mixture was cooled and treated with CH₂Cl₂. The insoluble red crystals of **22** were isolated by filtration and dried under vacuum. Yield, 40–45 %; m.p. >260 °C; ¹H NMR (CDCl₃), δ = 2.03 (br s, 12 H, Me), 2.19 (m, 12 H, Me), 7.40 (br s, 20 H, Ph); ³¹P NMR, δ = -1 1.6; MS (70 eV), *m/z* 744 (M, 100 %), 558 (M - C₁₂H₁₁P, 41 %), 372 (M/2, 50 %).

Synthesis of 1-phenyl-2,5-di(2-thienyl)phosphole (**35d**) (Scheme 4.10) [15a]

To a THF solution (40 mL) of Cp₂ZrCl₂ (1.08 g, 3.70 mmol) was added dropwise, at -78 °C, a hexane solution of 2.5 M *n*-BuLi (3.10 mL, 7.70 mmol). The reaction mixture was stirred for 1 h at -78 °C and a THF solution (20 mL) of 1,8-di(2-thienyl)octadiyne (0.81 mL, 3.70 mmol) was added dropwise at this temperature. The solution was allowed to warm to room temperature and stirred for 12 h. To this solution was added, at -78 °C, freshly distilled PhPBr₂ (0.77 mL, 3.70 mmol). The solution was allowed to warm to room temperature and stirred for 4 h at 40 °C. The solution was filtered and the volatile materials were removed *in vacuo*. Compound **35d** was isolated as an orange solid after purification on basic alumina (THF). Yield, 1.05 g, 75 %; *R_F* (alumina, THF) = 0.7; m.p. 134 °C; ¹H NMR (CD₂Cl₂): δ = 1.85 (m, 4H, C=CCH₂CH₂), 2.90 (m, 4H, C=CCH₂), 6.95 [ddd, ³*J*(H,H) = 5.1 and 3.7 Hz, ⁵*J*(P,H) = 1.0 Hz, 2H, H₄ thio], 7.08 [ddd, ³*J*(H,H) = 3.7 and ⁴*J*(H,H) = 1.1 Hz, ⁴*J*(P,H) = 0.4 Hz, 2H, H₃ thio], 7.23 [ddd, ³*J*(H,H) = 5.1 and ⁴*J*(H,H) = 1.1 Hz, ⁶*J*(P,H) = 1.2 Hz, 2H, H₅ thio], 7.25 (m, 3H, H_{m,p} Ph), 7.46 [ddd, ³*J*(H,H) = 7.8 and 1.6 Hz, ³*J*(P,H) = 7.8 Hz, 2H, H_o Ph]; ¹³C{¹H} (CDCl₃), δ = 23.1 (s, C=CCH₂CH₂), 29.3 (s, C=CCH₂), 124.8 [d, ⁵*J*(P,C) = 2.0 Hz, C₅ thio], 125.6 [d, ³*J*(P,C) = 10.0 Hz, C₃ thio], 126.8 (s, C₄ thio), 128.7 [d, ³*J*(P,C) = 9.0 Hz, C_m Ph], 129.6 (s, C_p Ph), 133.5 [d, ¹*J*(P,C) = 13.0 Hz, C_i Ph], 133.9 [d, ²*J*(P,C) = 19.0 Hz, C_o Ph], 135.7 (s, PC=C), 139.7 [d, ²*J*(P,C) = 22.0 Hz, C₂ thio], 144.4 [d, ²*J*(P,C) = 9.0 Hz, PC=C]; ³¹P-{¹H} (CDCl₃), δ = +12.7; HRMS (EI), *m/z* found 378.0651 *M*⁺; C₂₂H₁₉PS₂ calcd 378.0666; elemental analysis, calcd for C₂₂H₁₉PS₂ (378.49) C 69.82, H 5.06; found C 69.93, H 5.31 %.

Synthesis of polymer **81** (Scheme 4.23) [57c]

Catalytic amounts of [Pd(PPh₃)₄] (chiffres?) and CuI were added to a solution of dithienophosphole **80** (1.73 g, 1.5 mmol) and 1,4-diiodo-2,5-bis(octyloxy)benzene (0.88 g, 1.5 mmol) in *N*-methylpyrrolidinone (80 mL). The light-yellow reaction mixture was then stirred for 48 h at 200 °C, after which time the color changed to orange-red. The solution was then cooled to room temperature, the solvent evaporated under vacuum and the resulting amorphous solid taken up in a small amount of THF (ca. 5 mL). The suspension was filtered, precipitated into hexane and the residue dried under vacuum to yield **80** as a reddish brown pow-

der (1.1 g). $^{31}\text{P}\{^1\text{H}\}$ NMR ($\text{C}_2\text{D}_2\text{Cl}_4$), $\delta \approx 14$ ppm; ^1H NMR ($\text{C}_2\text{D}_2\text{Cl}_4$), $\delta \approx 7.64$ – 6.90 (br, Ar-H), 3.95 (br, OCH_2), 1.71–0.88 ppm (br m, alkyl-H); $^{13}\text{C}\{^1\text{H}\}$ NMR ($\text{C}_2\text{D}_2\text{Cl}_4$), $\delta \approx 155.6$, 144.0, 142.1, 130.5, 128.4 (br, C_{Ar}), 69.6 (br, OCH_2), 31.6, 29.1, 26.6, 26.1, 22.5, 14.1, 13.5 ppm (C_{alkyl}).

Synthesis of phosphonium salt **136** (Scheme 4.39) [73a]

Tris[4-(*N,N*-dibutylamino)azobenzene-4'-yl]phosphane (105 mg, 0.11 mmol), 4-(*N,N*-dibutylamino)-4'-iodoazobenzene (48 mg, 0.11 mmol) and $\text{Pd}(\text{OAc})_2$ (0.4 mg, 0.0018 mmol) were stirred with 1.5 mL of oxygen-free, nitrogen-saturated *p*-xylene under an inert atmosphere for 20 h at 140 °C, resulting in the separation of a dark-red oil. The xylene solution was removed with a pipette and the residue purified by chromatography on silica gel with ethyl acetate–MeOH (10:0.5) as eluent. A concentrated solution of the product in CH_2Cl_2 was dropped into vigorously stirred petroleum ether. The dark-red precipitate was collected by filtration and dried *in vacuo*. Yield, 74 mg (48 %); ^1H NMR (CDCl_3), $\delta = 8.09$ (m, 8H, H3/5), 7.90 (m, 8H, H2'/6'), 7.75 (m, 8H, H2/6), 6.71 (m, 8H, H3'/5'), 3.41 (m, 16H, α -H), 1.65 (m, 16H, β -H), 1.40 (m, 16H, α -H), 0.99 (t, $J = 7.2$ Hz, 24H, δ -H); $^{13}\text{C}\{^1\text{H}\}$ NMR (CDCl_3), $\delta = 157.9$ [d, $J(\text{C},\text{P}) = 3.3$ Hz, C4], 152.3 (C1'), 143.5 (C4'), 135.4 [d, $J(\text{C},\text{P}) = 11.1$ Hz, C2/6], 126.8 (C2'/6'), 123.8 [d, $J(\text{C},\text{P}) = 13.7$ Hz, C3/5], 116.2 [d, $J(\text{C},\text{P}) = 92.2$ Hz, C1], 111.4 (C3'/5'), 51.1 (α -C), 29.6 (β -C), 20.3 (γ -C), 13.9 (δ -C); elemental analysis, calcd for $\text{C}_{80}\text{H}_{104}\text{IN}_{12}\text{P}\cdot\text{H}_2\text{O}$ (1409.69), C 68.16, H 7.58, N 11.92; found, C 68.17, H 7.58, N 11.66 %; MS (PI-LSIMS), m/z 1263 (100 %, K^+), 1571 (30 %, [K.dibutylaminoazobenzényl]); HRMS (FAB), calcd 1263.82140 (K), found 1263.82446.

Synthesis of polymer **144** (Scheme 4.41) [78]

All glassware was rinsed with Me_3SiCl and flame dried prior to use. Compounds **142** (0.601 g, 2.32 mmol) and **143** (1.00 g, 2.32 mmol) were mixed as finely ground powders and flame sealed *in vacuo* in a thick-walled Pyrex tube. The sample was placed in a preheated (85 °C) oven, whereupon the solids melted forming a colorless, free-flowing liquid. After 6–8 h, the mixture showed an increase in viscosity and was yellow. The reaction was monitored until the liquid was almost immobile (ca. 24 h) and the yellow–orange material was removed from the oven. The tube was broken, Me_3SiCl was removed *in vacuo* and the residue was dissolved in a minimum amount of THF (ca. 3 mL). The viscous solution was evenly distributed over the walls of the flask and cold hexane (ca. –30 °C) was added rapidly to precipitate the polymer as a yellow solid. The hexane-soluble fraction was removed, leaving polymer **144** (0.384 g, 35 %) as a bright-yellow, glassy solid after drying *in vacuo*. ^{31}P NMR (CDCl_3), $\delta = 157$ – 149 [br m, (*E*)-**144**], 138–124 [br m, (*Z*)-**144**], –137 ppm [br, P(SiMe_3)₂ end groups]; ^{29}Si NMR (CDCl_3), $\delta = 21.7$ – 20.5 (br m), 18.4–17.0 (br m), 1.4 ppm [d; $^1J(\text{Si}, \text{P}) = 26$ Hz, end groups]; ^1H NMR (CDCl_3), $\delta = 7.8$ – 6.6 (br m; C_6H_4), 2.5–2.1 [br m, $\text{C}_6(\text{CH}_3)_4$], 0.5–0.5 [br m, $\text{Si}(\text{CH}_3)_3$]; $^{13}\text{C}\{^1\text{H}\}$ NMR (CDCl_3), $\delta = 211.9$ [br, (*Z*)-C=P], 197.9 [br, (*E*)-C=P], 142.0 (br, *i*- C_6Me_4), 139.1 (br, *i*- C_6H_4), 132.4, 130.2 (br, *o*- C_6H_4 , *o*- C_6Me_4), 18.6,

17.5 [br s, C₆(CH₃)₄], 0.7, 0.2 [br s, OSi(CH₃)₃]; IR (film), ν = 2955 (m), 2921 (m), 2849 (m), 1252 (vs), 1187 (s), 846 (vs).

Synthesis of polymer **156c** (Scheme 4.43) [80d]

To a solution of **155** (0.200 g; 0.171 mmol) in THF (15 mL) was added a solution of 2,5-thiophenedicarboxaldehyde (0.0241 g; 0.172 mmol) in THF (15 mL) over 1 h. Over the course of addition the reaction mixture changed progressively from violet to bright orange. After stirring overnight, additional 2,5-thiophenedicarboxaldehyde (0.0241 g) was added to quench any unreacted -P=PMe₃ end groups. Volatile components were removed *in vacuo* and the crude orange solid was rinsed with MeCN and *n*-pentane to yield **155** (0.178 g, 85.4%). ¹H NMR (C₆D₆), δ = 0.84 (t, 6H, *J* = 7 Hz), 1.20–1.40 (m, 8H), 1.40–1.55 (m, 4H), 1.75–1.90 (m, 4H), 2.04 (s, 24H), 2.09 (s, 3.7H, end group), 2.30 (s, 12H), 2.35 (s, 1.8H, end group), 4.00 (t, 4H, *J* = 7 Hz), 6.31 (s, 2H), 6.88 (s, 8H), 6.92 (s, 1.2H, end group), 7.05 (s, 2H), 7.08–7.21 (m, 2H), 7.23 (s, 4H), 7.40–7.55 (m, 2H), 8.28 (d, 2H, *J* = 20 Hz), 8.42 (d, 0.3H, *J* = 23 Hz, end group), 9.73 (s, 0.6H, terminal -CHO); ³¹P NMR (CDCl₃), δ = 232.3 (s, internal P=C), 256.8 (s, terminal P=C).

Synthesis of diphosphene polymer **157** (Scheme 4.43) [80d]

A sample of **155** (0.10 g, 0.050 mmol) was heated under nitrogen at ~250° C for 2 min, during which time the material melted as it changed color from violet to red and a vapor was emitted. The material was cooled to room temperature, leaving a hard, transparent, red solid. The solid was stirred with acetonitrile (5 mL) to produce a fine suspension of the material, which was isolated by filtration and the solid dried *in vacuo* to give 0.091 g (99%) of **155** as a red powder. ¹H NMR (C₆D₆), δ = 0.82 (br, 6H), 1.14 (br, 8H), 1.32 (br, 4H), 1.53 (br, 4H), 1.96 (s, 24H), 2.21 (s, 12H), 3.73 (br, 4H), 6.81 (s, 8H), 7.09–7.23 (br m, 4H), 7.31 (s, 4H), 7.84 (d, 2H, *J* = 15 Hz); ³¹P NMR (CDCl₃), δ = 493.5 (broad).

References

1. (a) A. Kraft, A. C. Grimsdale, A. B. Holmes, *Angew. Chem. Int. Ed.* **1998**, *37*, 402; (b) U. Mitschke, P. Bäuerle, *J. Mater. Chem.* **2000**, *10*, 1471; (c) A. P. Kulkarni, C. J. Tonzola, A. Babel, S. A. Jenekhe, *Chem. Mater.* **2004**, *16*, 4556; (d) C.-T. Chen, *Chem. Mater.* **2004**, *16*, 4389; (e) B. W. D'Andrade, S. R. Forrest, *Adv. Mater.* **2004**, *16*, 1585.
2. (a) K. Müllen, G. Wegner, *Electronic Materials: the Oligomer Approach*, Wiley-VCH, Weinheim, **1998**; (b) G. H. Geinck, T. C. T. Geuns, D. M. de Leeuw, *Appl. Phys. Lett.* **2000**, *77*, 1487; (c) B. K. Crone, A. Dodabalapur, R. Sarpeshkar, A. Gelperin, H. E. Katz, Z. Bao, *J. Appl. Phys.* **2002**, *91*, 10140; (d) J. A. Rogers, Z. Bao, H. E. Katz, A. Dodabalapur, in *Thin-film Transistors*, C. R. Kagan, P. Andry (Eds.), Marcel Dekker, New York, **2003**, p. 377; (e) V. C. Sundar, J. Zaumseil, V. Podzorov, E. Menard, R. L. Willett, T. Someya, M. E. Gershenson, J. A. Rogers, *Science* **2004**, *303*, 1644; (f) Z. Bao, *Nat. Mater.* **2004**, *3*, 137; (g) N. Stutzmann, R. H. Friend, H. Sirringhaus, *Science* **2003**, *299*, 1881; (h) F. Garnier, R. Hajlaoui, A. Yassar, P. Srivastava, *Science* **1994**, *265*, 1684; (i) G. H. Gelinck, H. E. A. Huitema, E. van Veenendaal, E. Cantatore, L. Schrijnemakers, J. B. P. H. van der Putten, T. C. T. Geuns, M. Beenhakkers, J. B. Giesbers, B.-H. Huisman, E. J. Meijer, E. M. Benito, F. J. Touwslager, A. W. Marsman, B. J. E. van Rens, D. M. de Leeuw, *Nat. Mater.* **2004**, *3*, 106; (j) S. R. Forrest, *Nature* **2004**, *428*, 911; (k) E. J. Meijer, D. M. De Leeuw, S. Setayesh, E. van Veenendaal, B.-H. Huisman, P. W. M. Blom, J. C. Hummelen, U. Scherf, T. M. Klapwijk, *Nat. Mater.* **2003**, *2*, 678.
3. See, for example. (a) <http://www.kodak.com/US/en/corp/display/index.jhtml>; (b) <http://www.research.philips.com/technologies/display/>; (c) <http://www.dupont.com/displays/oled/>; (d) <http://www.cdtdtd.co.uk/>; (e) <http://www.universaldisplay.com/>; (f) <http://www.covion.com/index.html>.
4. (a) C. W. Tang, S. A. Van Slyke, *J. Appl. Phys.* **1987**, *51*, 913; (b) C. W. Tang, S. A. Van Slyke, C. H. Chen, *J. Appl. Phys.* **1989**, *65*, 3610; (c) J. H. Burroughes, D. D. C. Bradley, A. R. Brown, R. N. Marks, K. Mackay, R. H. Friends, P. L. Burns, A. B. Holmes, *Nature* **1990**, *347*, 539; (d) M. A. Baldo, D. F. O'Brien, Y. You, A. Shoustikov, S. Sibley, M. E. Thompson, S. R. Forrest, *Nature* **1998**, *395*, 151.
5. (a) R. E. Martin, F. Diederich, *Angew. Chem. Int. Ed.* **1999**, *38*, 1350; (b) T. A. Skotheim, R. L. Elsenbaumer, J. R. Reynolds, *Handbook of Conducting Polymers* (2nd edn.), Marcel Dekker, New York, **1998**; (c) H. S. Nalwa, *Handbook of Conductive Materials and Polymers*, Wiley, New York, **1997**; (d) J. Roncali, *Chem. Rev.* **1997**, *97*, 173; (e) F. J. M. Hoeben, P. Jonkheijm, E. W. Meijer, A. P. H. J. Schenning, *Chem. Rev.* **2005**, *105*, 1491; (f) F. Badubri, G. M. Farinola, F. Naso, *J. Mater. Chem.* **2004**, *14*, 11; (g) P. F. H. Schwab, J. R. Smith, J. Michl, *Chem. Rev.* **2005**, *105*, 1197; (h) M. B. Nielsen, F. Diederich, *Chem. Rev.* **2005**, *105*, 1837; (i) S. Szafert, J. A. Gladysz, *Chem. Rev.* **2003**, *103*, 4175; (j) M. Hissler, P. W. Dyer, R. Réau, *Coord. Chem. Rev.* **2003**, *244*, 1; (k) U. H. F. Bunz, *Chem. Rev.* **2000**, *100*, 1605; (l) B. J. Holliday, T. M. Swager, *Chem. Commun.* **2005**, 23.
6. (a) D. L. Albert, T. J. Marks, M. A. Ratner, *J. Am. Chem. Soc.* **1997**, *119*, 6575; (b) U. Salzner, J. B. Lagowski, P. G. Pickup, R. A. Poirier, *Synth. Met.* **1998**, *96*, 177; (c) J. Ma, S. Li, Y. Jiang, *Macromolecules* **2002**, *35*, 1109.
7. (a) F. Mathey, *Phosphorus–Carbon Heterocyclic Chemistry: the Rise of a New Domain*, Elsevier Science, Oxford, **2001**; (b) K. Dillon, F. Mathey, J. F. Nixon, *Phosphorus: the Carbon Copy*, Wiley, Chichester, **1998**; (c) L. Nyulaszi, *Chem. Rev.* **2001**, *101*, 1229; (d) F. Mathey, *Angew. Chem. Int. Ed.* **2003**, *42*, 1578.
8. (a) H. R. Allcock, *Chemistry and Applications of Polyphosphazenes*, Wiley-Interscience, New York, **2003**; (b) M. Gleria, R. De Jaeger, *Top. Curr. Chem.* **2005**, *250*, 165–251; (c) M. Escobar, Z. Jin, B. L. Lucht, *Org. Lett.* **2002**, *13*, 2213.

9. First dibenzophosphole (a) G. Wittig, G. Geissler, *Liebigs Ann. Chem.* **1953**, 580, 44; first phospholes (b) E. H. Bray, W. Hübel, *Chem. Ind. (London)* **1959**, 1250; (c) E. H. Bray, W. Hübel, I. Caplier *J. Am. Chem. Soc.* **1961**, 83, 4406.
10. (a) F. Mathey, *Chem. Rev.* **1988**, 88, 429; (b) L. D. Quin, in *Phosphorus–Carbon Heterocyclic Chemistry: the Rise of a New Domain*, F. Mathey (Ed.), Elsevier Science, Oxford, **2001**, pp. 217, 307; (c) C. Charrier, H. Bonnard, G. de Lauzon, F. Mathey, *J. Am. Chem. Soc.* **1983**, 105, 6871; (d) F. Mathey, *Acc. Chem. Res.* **2004**, 37, 954.
11. (a) P. v. R. Schleyer, C. Maerker, A. Dransfeld, H. Jiao, N. J. R. van Eikema Hommes, *J. Am. Chem. Soc.* **1996**, 118, 6317; (b) P. v. R. Schleyer, P. K. Freeman, H. Jiao, B. Goldfuss, *Angew. Chem. Int. Ed.* **1995**, 34, 337.
12. (a) W. Egan, R. Tang, G. Zon, K. Mislow, *J. Am. Chem. Soc.* **1971**, 93, 6205; (b) D. Delaere, A. Dransfeld, M. T. Nguyen, L. G. Vanquickenborne, *J. Org. Chem.* **2000**, 65, 2631.
13. (a) W. Schäfer, A. Schweig, F. Mathey, *J. Am. Chem. Soc.* **1976**, 98, 407; (b) E. Mattmann, F. Mathey, A. Sevin, G. Frison, *J. Org. Chem.* **2002**, 67, 1208.
14. (a) S. Yamaguchi, K. Tamao, *J. Chem. Soc., Dalton Trans.* **1998**, 3693; (b) F. Wang, J. Luo, K. Yang, J. Chen, F. Huang, Y. Cao, *Macromolecules* **2005**, 38, 2253; (c) S. Yamaguchi, K. Tamao, *Chem. Lett.* **2005**, 34, 2; (d) A. J. Boydston, B. L. Pagenkopf, *Angew. Chem. Int. Ed.* **2004**, 43, 6336; (e) A. J. Boydston, J. Andrew, Y. Yin, B. L. Pagenkopf, *J. Am. Chem. Soc.* **2004**, 126, 10350.
15. (a) C. Hay, M. Hissler, C. Fischmeister, J. Rault-Berthelot, L. Toupet, L. Nyulaszi, R. Réau, *Chem. Eur. J.* **2001**, 7, 4222; (b) J. Hydrio, M. Gouygou, F. Dallemer, G. G. A. Balavoine, J.-C. Daran, *Eur. J. Org. Chem.* **2002**, 675; (c) X. Sava, N. Mézaille, N. Maigrot, F. Nief, L. Ricard, F. Mathey, P. Le Floch, *Organometallics* **1999**, 18, 4205.
16. A. Brèque, G. Muller, H. Bonnard, F. Mathey, P. Savignac, *Eur. Pat.* 41447, **1981**.
17. (a) F. Mercier, F. Mathey, J. Fischer, J. H. Nelson, *Inorg. Chem.* **1985**, 24, 4141; (b) F. Mercier, F. Mathey, J. Fischer, J. H. Nelson, *J. Am. Chem. Soc.* **1984**, 106, 425.
18. (a) F. Mercier, S. Holand, F. Mathey, *J. Organomet. Chem.* **1986**, 316, 271; (b) O. Tissot, J. Hydrio, M. Gouygou, F. Dallemer, J.-C. Daran, G. G. A. Balavoine, *Tetrahedron* **2000**, 56, 85; (c) O. Tissot, M. Gouygou, J.-C. Daran, G. G. A. Balavoine, *Chem. Commun.* **1996**, 2287.
19. E. Deschamps, F. Mathey, *Bull. Soc. Chim. Fr.* **1992**, 129, 486.
20. T.-A. Niemi, P. L. Coe, S. J. Till, *J. Chem. Soc., Perkin Trans.* **2000**, 1519.
21. E. Deschamps, L. Ricard, F. Mathey, *Angew. Chem. Int. Ed. Engl.* **1994**, 33, 1158.
22. (a) M. Gouygou, O. Tissot, J.-C. Daran, G. G. A. Balavoine, *Organometallics* **1997**, 16, 1008; (b) J. Hydrio, M. Gouygou, F. Dallemer, G. G. A. Balavoine, J.-C. Daran, *Tetrahedron: Asymmetry* **2002**, 13, 1097; (c) J. Hydrio, M. Gouygou, F. Dallemer, J.-C. Daran, G. G. A. Balavoine, *Eur. J. Org. Chem.*, **2002**, 675; (d) O. Tissot, M. Gouygou, J.-C. Daran, G. G. A. Balavoine, *Organometallics*, **1998**, 17, 5927; (e) O. Tissot, M. Gouygou, F. Dallemer, J.-C. Daran, G. G. A. Balavoine, *Eur. J. Inorg. Chem.* **2001**, 2385; (f) T. Kojima, K. Saeki, K. Ono, Y. Matsuda, *Bull. Chem. Soc. Jpn.* **1998**, 71, 2885; (g) O. Tissot, M. Gouygou, F. Dallemer, J.-C. Daran, G. G. A. Balavoine, *Angew. Chem. Int. Ed.* **2001**, 40, 1076.
23. (a) E. W. Abel, C. Towers, *J. Chem. Soc., Dalton Trans.* **1979**, 814; (b) C. Charrier, H. Bonnard, F. Mathey, *J. Org. Chem.* **1982**, 47, 2376; (c) C. Charrier, H. Bonnard, F. Mathey, D. Neibecker, *J. Organomet. Chem.* **1982**, 231, 361; (d) S. Holand, F. Mathey, J. Fischer, A. Mitschler, *Organometallics* **1983**, 2, 1234; (e) J. K. Vohs, P. Wie, J. Su, B. C. Beck, S. D. Goodwin, G. H. Robinson, *Chem. Commun.* **2000**, 1037.
24. (a) D. Carmichael, F. Mathey, *Top. Curr. Chem.* **2002**, 220, 27–51; (b) F. Mathey, *J. Organomet. Chem.* **2002**, 646, 15; (c) F. Nief, *Eur. J. Inorg. Chem.* **2001**, 4, 891; (d) C. Ganter, *J. Chem. Soc., Dalton*

- Trans.* **2001**, 3541; (e) N. M. Kostic, R. F. Fenske *Organometallics* **1983**, *2*, 1008; (f) G. Frison, F. Mathey, A. Sevin, *J. Phys. Chem. A* **2002**, *106*, 5653; (g) D. Turcitu, F. Nief, L. Ricard, *Chem. Eur. J.* **2003**, *9*, 4916; (h) R. Shintani, G. C. Fu, *J. Am. Chem. Soc.* **2003**, *125*, 10778; (i) L. Weber, *Angew. Chem. Int. Ed.* **2002**, *41*, 563; (j) M. Ogasawara, T. Nagano, T. Hatashi, *Organometallics* **2003**, *22*, 1174; (k) L.-S. Wang, T. K. Hollis, *Org. Lett.* **2003**, *5*, 2543; (l) X. Sava, M. Melaimi, L. Ricard, F. Mathey, P. Le Floch, *New J. Chem.* **2003**, *27*, 1233; (m) G. de Lauzon, B. Deschamps, J. Fischer, F. Mathey, A. Mitschler, *J. Am. Chem. Soc.* **1980**, *102*, 994; (n) X. Sava, L. Ricard, F. Mathey, P. Le Floch, *Organometallics* **2000**, *19*, 4899.
- 25.** C. Fave, M. Hissler, T. Karpati, J. Rault-Berthelot, V. Deborde, L. Toupet, L. Nyulaszi, R. Réau, *J. Am. Chem. Soc.* **2004**, *126*, 6058.
- 26.** (a) R. Hoffmann, *Acc. Chem. Res.* **1971**, *4*, 1; (b) R. Hoffmann, A. Imamura, W. J. Hehre, *J. Am. Chem. Soc.* **1968**, *90*, 1499; (c) M. N. Paddon-Row, *Acc. Chem. Res.* **1994**, *27*, 18; (d) R. Gleiter, W. Schäfer, *Acc. Chem. Res.* **1990**, *23*, 369; (e) B. P. Paulson, L. A. Curtiss, B. Bal, G. L. Closs, J. R. Miller, *J. Am. Chem. Soc.* **1996**, *118*, 378.
- 27.** (a) S. Yamaguchi, K. Tamao, in *The Chemistry of Organic Silicon Compounds*, Z. Rappoport, T. Appeloig (Eds.), Wiley, New York, **2001**, Vol. 3, p. 647; (b) S. Yamaguchi, R.-Z. Jin, K. Tamao, *J. Am. Chem. Soc.* **1999**, *121*, 2937; (c) H. Sohn, M. J. Sailor, D. Madge, W. C. Trogler, *J. Am. Chem. Soc.* **2003**, *125*, 3821; (d) H. Sohn, R. M. Calhoun, M. J. Sailor, W. C. Trogler, *Angew. Chem. Int. Ed.* **2001**, *40*, 2104; (e) T. Sanji, T. Sakai, C. Kabuto, H. Sakurai, *J. Am. Chem. Soc.* **1998**, *120*, 4552; (f) H. Sohn, R. R. Huddleston, D. R. Power, R. West, *J. Am. Chem. Soc.* **1999**, *121*, 2935; (g) A. Rose, Z. Zhu, C. F. Madigan, T. M. Swager, V. Bulovic, *Nature* **2005**, *434*, 7035.
- 28.** (a) F. Mathey, F. Mercier, F. Nief, J. Fischer, A. Mitschler, *J. Am. Chem. Soc.* **1982**, *104*, 2077; (b) F. J. Fischer, A. Mitschler, F. Mathey, F. Mercier, *J. Chem. Soc., Dalton Trans.* **1983**, 841; (c) F. Laporte, F. Mercier, L. Ricard, F. Mathey, *J. Am. Chem. Soc.* **1994**, *116*, 3306.
- 29.** (a) E. Deschamps, L. Ricard, F. Mathey, *Heteroat. Chem.* **1991**, *2*, 377; (b) E. Deschamps, F. Mathey, *J. Org. Chem.* **1990**, *55*, 2494.
- 30.** (a) P. J. Fagan, W. A. Nugent, *J. Am. Chem. Soc.* **1988**, *110*, 2310; (b) P. J. Fagan, W. A. Nugent, J. C. Calabrese, *J. Am. Chem. Soc.* **1994**, *116*, 1880.
- 31.** (a) D. Le Vilain, C. Hay, V. Deborde, L. Toupet, R. Réau, *Chem. Commun.* **1999**, 345; (b) C. Hay, C. Fischmeister, M. Hissler, L. Toupet, R. Réau, *Angew. Chem. Int. Ed.* **2000**, *39*, 1812; (c) M. Sauthier, F. Leca, L. Toupet, R. Réau, *Organometallics* **2002**, *21*, 1591; (d) C. Hay, M. Sauthier, V. Deborde, M. Hissler, L. Toupet, R. Réau, *J. Organomet. Chem.* **2002**, *643–644*, 494; (f) C. Fave, M. Hissler, K. Sénéchal, I. Ledoux, J. Zyss, R. Réau, *Chem. Commun.* **2002**, 1674.
- 32.** D. Delaere, M. T. Nguyen, L. G. Vanquickenborne, *J. Phys. Chem. A* **2003**, *107*, 838.
- 33.** (a) A. Hucke, M. P. Cava, *J. Org. Chem.* **1998**, *63*, 7413; (b) P. E. Niziurski-Mann, C. C. Scordilis-Kelley, T. L. Liu, M. P. Cava, R. T. Carlin, *J. Am. Chem. Soc.* **1993**, *115*, 887; (c) S. Yamaguchi, Y. Itami, K. Tamao, *Organometallics* **1998**, *17*, 4910.
- 34.** C. Fave, T. Y. Cho, M. Hissler, C. W. Chen, T. Y. Luh, C. C. Wu, R. Réau, *J. Am. Chem. Soc.* **2003**, *125*, 9254.
- 35.** (a) H. Schmidbaur, *Gold Bull.* **1990**, *23*, 11; (b) P. Pyykkö, *Chem. Rev.* **1997**, *97*, 597; (c) P. Pyykkö, *Angew. Chem. Int. Ed.*, **2004**, *43*, 4412; (d) W. W. Yam, K. W. Lo, W. K. M. Fung, C. R. Wang, *Coord. Chem. Rev.* **1998**, *171*, 17.
- 36.** (a) T.-H. Liu, C.-Y. Iou, C. H. Chen, *Appl. Phys. Lett.* **2003**, *83*, 5241; (b) R. H. Young, C. W. Tang, A. P. Marchetti, *Appl. Phys. Lett.* **2002**, *80*, 874; (c) J. Feng, F. Li, W. Gao, G. Cheng, W. Xie, S. Liu, *Appl. Phys. Lett.* **2002**, *81*, 2935.
- 37.** C. Hay, C. Fave, M. Hissler, J. Rault-Berthelot, R. Réau, *Org. Lett.* **2003**, *19*, 3467.
- 38.** J. W. Sease, L. Zechmeister, *J. Am. Chem. Soc.* **1947**, *69*, 270.

39. (a) C. Adachi, M. A. Baldo, S. R. Forrest, S. Lamansky, M. E. Thompson, R. C. Kwong, *Appl. Phys. Lett.* **2001**, *78*, 1622; (b) R. J. Holmes, S. R. Forrest, Y. J. Tung, R. C. Kwong, J. J. Brown, S. Garon, M. E. Thompson, *Appl. Phys. Lett.* **2003**, *82*, 2422.
40. (a) C. Denault, I. Ledoux, I. D. W. Samuel, J. Zyss, M. Bourgault, H. Le Bozec, *Nature* **1995**, *374*, 339; (b) K. Sénéchal, O. Maury, H. Le Bozec, I. Ledoux, J. Zyss, *J. Am. Chem. Soc.* **2002**, *124*, 4560; (c) L. Viau, S. Bidault, O. Maury, S. Brasselet, I. Ledoux, J. Zyss, E. Ishow, K. Nakatani, H. Le Bozec, *J. Am. Chem. Soc.* **2004**, *126*, 8386; (d) O. Maury, H. Le Bozec, *Acc. Chem. Res.* **2005**, *38*, 691.
41. (a) C. Hay, M. Sauthier, V. Deborde, M. Hissler, L. Toupet, R. Réau, *J. Organomet. Chem.* **2002**, *643–644*, 494; (b) M. Sauthier, B. Le Guennic, V. Deborde, L. Toupet, J.-F. Halet, R. Réau, *Angew. Chem. Int. Ed.* **2001**, *40*, 228; (c) F. Leca, M. Sauthier, V. Deborde, L. Toupet, R. Réau, *Chem. Eur. J.* **2003**, *16*, 3785; (d) F. Leca, C. Lescop, E. Rodriguez, K. Costuas, J.-F. Halet, R. Réau, *Angew. Chem. Int. Ed.* **2005**, *44*, 2190.
42. (a) R. G. Pearson, *Inorg. Chem.* **1973**, *12*, 712; (b) M. Sauthier, F. Leca, L. Toupet, R. Réau, *Organometallics* **2002**, *21*, 1591; (c) F. Leca, C. Lescop, R. Réau, *Organometallics* **2004**, *23*, 6191; (d) C. Fave, M. Hissler, K. Sénéchal, I. Ledoux, J. Zyss, R. Réau, *Chem. Commun.* **2002**, 1674.
43. (a) O. M. Bevierre, F. Mercier, L. Ricard, F. Mathey, *Angew. Chem. Int. Ed.* **1990**, *29*, 655; (b) M. O. Bevierre, F. Mercier, F. Mathey, A. Jutand, C. Amatore, *New J. Chem.* **1991**, *15*, 545.
44. E. Deschamps, L. Ricard, F. Mathey, *J. Chem. Soc., Chem. Commun.* **1995**, 1561.
45. (a) J. J. Apperloo, J. M. Raimundo, P. Frère, J. Roncali, R. A. Janssen, *Chem. Eur. J.* **2000**, *9*, 1698; (b) I. Jestin, P. Frère, P. Blanchard, J. Roncali, *Angew. Chem. Int. Ed.* **1998**, *37*, 942; (c) S. Zahn, T. M. Swager, *Angew. Chem. Int. Ed.* **2002**, *41*, 4225.
46. For examples: (a) H. Jiao, K. Costuas, J. A. Gladysz, J.-F. Halet, M. Guillemot, L. Toupet, F. Paul, C. Lapinte, *J. Am. Chem. Soc.* **2003**, *125*, 9511; (b) Z. Zhu, T. M. Swager, *J. Am. Chem. Soc.* **2002**, *124*, 9670; (c) C. A. Breen, T. Deng, T. Breiner, E. L. Thomas, T. M. Swager, *J. Am. Chem. Soc.* **2003**, *125*, 9942.
47. (a) S. Holand, F. Gandolfo, L. Ricard, F. Mathey, *Bull. Soc. Chim. Fr.* **1996**, *33*, 133; (b) T.-A. Niemi, P. L. Coe, S. J. Till, *J. Chem. Soc., Perkin Trans.* **2000**, 519.
48. (a) S. S. H. Mao, T. D. Tilley, *Macromolecules* **1997**, *30*, 5566; (b) B. L. Lucht, S. S. H. Mao, T. D. Tilley, *J. Am. Chem. Soc.* **1998**, *120*, 4354; (c) B. L. Lucht, T. D. Tilley, *Chem. Commun.* **1998**, 1645.
49. (a) T. Takahashi, *Jpn. Pat.* 2003261585, **2003**; (b) Y. Morisaki, Y. Aiki, Y. Chujo, *Macromolecules* **2003**, *36*, 2594.
50. (a) P. Audebert, J.-M. Catel, G. Le Coustumer, V. Duchenet, P. Hapiot, *J. Phys. Chem. B* **1998**, *102*, 8661; (b) P. Audebert, J.-M. Catel, V. Duchenet, L. Guyard, P. Hapiot, G. Le Coustumer, *Synth. Met.* **1999**, *101*, 642.
51. (a) A. N. Hughes, D. Kleemola, *J. Heterocycl. Chem.* **1976**, *13*, 1; (b) W. Egan, R. Tang, G. Zon, K. Mislou, *J. Am. Chem. Soc.* **1971**, *93*, 6205.
52. S. Kobayashi, M. Noguchi, Y. Tsubata, M. Kitano, H. Doi, T. Kamioka, A. Nakazono, *Jpn. Pat.* 2003231741, **2003**.
53. (a) E. Duran, E. Gordo, J. Granell, D. Velasco, F. Lopez-Calahorra, *Tetrahedron Lett.* **2001**, *42*, 7791; (b) E. Duran, D. Velasco, F. Lopez-Calahorra, H. Finkelmann, *Mol. Cryst. Liq. Cryst.* **2002**, *381*, 43.
54. M. Taillefer, F. Plenat, C. Combes-Chamalet, V. Vicente, H. J. Cristau, *Phosphorus Res. Bull.* **1999**, *10*, 696.
55. J.-P. Lampin, F. Mathey, *J. Organomet. Chem.* **1974**, *71*, 239.
56. (a) S. Kim, K.-H. Song, S. O. Kang, J. Ko, *Chem. Commun.* **2004**, 68; (b) K. Ogawa, S. C. Rasmussen, *J. Org. Chem.* **2003**, *68*, 2921; (c) J. Ohshita, M. Nodono, T. Watanabe, Y. Ueno, A. Kunai, Y. Harima, K. Yamashita, M. Ishikawa, *J. Organomet. Chem.* **1998**, *553*, 487; (d) G. Barbarella, L. Favaretto, G. Sotgiu, L. Antolini, G. Gigli, R. Cingolati, A. Bongini, *Chem. Mater.* **2001**, *13*, 4112; (e) G. Barbarella, M. Melucci, G. Sotgiu, *Adv. Mater.* **2005**, *17*, 1581.

57. (a) T. Baumgartner, *Macromol. Symp.* **2003**, *196*, 279; (b) T. Baumgartner, T. Neumann, B. Wirges, *Angew. Chem. Int. Ed.* **2004**, *43*, 6197; (c) T. Baumgartner, W. Bergmans, T. Karpati, T. Neumann, M. Nieger, L. Nuyalasz, *Eur. J. Chem.* **2005**, *11*, 4684.
58. (a) A. G. MacDiarmid, J. C. Chiang, A. J. Epstein, *Synth. Met.* **1987**, *18*, 285; (b) F. Wudl, R. O. Angus, Jr., F. L. Lu, P. M. Allemand, D. F. Vachon, M. Novak, Z. X. Liu, A. J. Heeger, *J. Am. Chem. Soc.* **1987**, *109*, 3677; (c) S. A. Hay, *Macromolecules* **1969**, *2*, 107; (d) R. H. Baughman, J. L. Bredas, R. R. Chance, R. L. Elsenbaumer, L. W. Shacklette, *Chem. Rev.* **1982**, *82*, 209; (e) F. E. Goodson, S. J. Hauck, J. F. Hartwig, *J. Am. Chem. Soc.* **1999**, *121*, 7527; (f) R. A. Singer, J. P. Sadighi, S. L. Buchwald, *J. Am. Chem. Soc.* **1998**, *120*, 213.
59. (a) B. L. Lucht, N. O. St. Onge, *Chem. Commun.* **2000**, 2097; (b) Z. Jin, B. L. Lucht, *J. Am. Chem. Soc.* **2005**, *127*, 5586.
60. (a) Z. Jin, B. L. Lucht, *J. Organomet. Chem.* **2002**, *653*, 167; (b) H. Ghassemi, E. McGrath, *Polymer* **1997**, *38*, 3139.
61. (a) F. E. Goodson, T. I. Wallow, B. M. Novak, *Macromolecules* **1998**, *31*, 2047; (b) F. E. Goodson, T. I. Wallow, B. M. Novak, *J. Am. Chem. Soc.* **1997**, *119*, 12441.
62. (a) D. K. Johnson, T. Rakuchaisirikul, Y. Sun, N. J. Taylor, A. J. Carty, A. J. Carty, N. J. Taylor, D. K. Johnson, *J. Am. Chem. Soc.* **1979**, *101*, 5422; (c) M. P. Martin-Redondo, L. Scoles, B. T. Sterenberg, K. A. Udachin, A. J. Carthy, *J. Am. Chem. Soc.* **2005**, *127*, 5038; (d) D. Xu, B. Hong, *Angew. Chem. Int. Ed.* **2000**, *39*, 1826; (e) J. Fornies, A. Garcia, J. Gomez, E. Lalinde, M. T. Moreno, *Organometallics* **2002**, *21*, 3733; (f) I. Ara, J. Fornies, A. Garcia, J. Gomez, E. Lalinde, M. T. Moreno, *Chem. Eur. J.* **2002**, *16*, 3698; (g) T. Baumgartner, K. Huynh, S. Schleidt, A. J. Lough, I. Manners, *Chem. Eur. J.* **2002**, *8*, 4622.
63. (a) P. J. Stang, F. Diederich, *Modern Acetylene Chemistry*, VCH, Weinheim, **1995**; (b) F. Diederich, P. J. Stang, R. R. Tykwinsky, *Acetylene Chemistry: Chemistry, Biology and Material Science*, VCH, Weinheim, **2005**.
64. L. T. Scott, M. Unno, *J. Am. Chem. Soc.* **1990**, *112*, 7823.
65. G. Märkl, T. Zollitsch, P. Kreitmeier, M. Prinzhorn, S. Reithinger, E. Eibler, *Chem. Eur. J.* **2000**, *6*, 3806.
66. V. Huc, A. Balueva, R.M. Sebastien, A.-M. Caminade, J.-P. Majoral, *Synthesis* **2000**, 726.
67. (a) S. Yamaguchi, S. Akiyama, K. Tamao, *J. Organomet. Chem.* **2002**, *646*, 277; (b) S. Yamaguchi, S. Akiyama, K. Tamao, *J. Am. Chem. Soc.* **2000**, *122*, 6793; (c) S. Yamaguchi, S. Akiyama, K. Tamao, *J. Am. Chem. Soc.* **2001**, *123*, 11372; (d) S. Yamaguchi, S. Akiyama, K. Tamao, *J. Organomet. Chem.* **2002**, *652*, 3.
68. (a) Y. Wang, M. I. Ranasinghe, T. Goodson, III, *J. Am. Chem. Soc.* **2003**, *125*, 9562; (b) M. Malagoli, J. Bredas, *Chem. Phys. Lett.* **2000**, *327*, 13; (c) R. C. Smith, J. D. Protasiewicz, *J. Chem. Soc., Dalton Trans.* **2000**, 4738; (d) R. C. Smith, M. J. Earl, J. D. Protasiewicz, *Inorg. Chim. Acta* **2004**, *357*, 4139; (e) Y. Kang, D. Song, H. Schmider, S. Wang, *Organometallics* **2002**, *21*, 2413.
69. L. G. Madrigal, C. W. Spangler, *Mater. Res. Soc. Symp. Proc.* **1999**, *561*, 75.
70. (a) T. Renouard, H. Le Bozec, *Eur. J. Inorg. Chem.* **2000**, *1*, 229; (b) S. Di Bella, *Chem. Soc. Rev.* **2001**, *30*, 355; (c) P. G. Lacroix, *Eur. J. Chem.* **2001**, 339.
71. (a) A. W. Johnson, W. C. Kaska, K. A. Astoja Stanzewski, D. A. Dixon, *Ylides and Imines of Phosphorus*, Wiley, New York, **1993**; (b) Y. G. Gololobov, L. F. Kasukhin, *Tetrahedron* **1992**, *48*, 1353.
72. K. V. Katti, K. Raghuraman, N. Pillarsetty, S. R. Kara, R. J. Gaulot, M. A. Chartier, C. A. Langhoff, *Chem. Mater.* **2002**, *14*, 2436.
73. (a) C. Lambert, E. Schmälzlin, K. Meerholz, C. Bräuchle, *Chem. Eur. J.* **1998**, *4*, 512; (b) C. Bourgogne, Y. Le Fur, P. Juen, P. Masson, J. F. Nicoud, R. Masse, *Chem. Mater.* **2000**, *12*, 1025.
74. (a) A. B. Padmaperuma, G. Schmett, D. Fogarty, N. Washton, S. Nanayakkara, L. Sapochak, K. Ashworth, L. Madrigal, B. Reeves, C. W. Spangler, *Mater. Res. Soc. Symp. Proc.* **2001**, *621*; (b) R. Métivier, R.

- Amengual, I. Leray, V. Michelet, J.-P. Genêt, *Org. Lett.*, **2004**, 6, 739.
75. (a) O. Clot, M. O. Wolf, B. O. Patrick, *J. Am. Chem. Soc.* **2000**, 122, 10456; (b) O. Clot, M. O. Wolf, B. O. Patrick, *J. Am. Chem. Soc.* **2001**, 123, 9963; (c) O. Clot, Y. Akahori, C. Moorlag, D. B. Leznoff, M. O. Wolf, R. J. Batchelor, B. O. Patrick, M. Ishii, *Inorg. Chem.* **2003**, 42, 2704.
76. (a) L. Nyulaszi, T. Veszpremi, J. Reffy, *J. Phys. Chem.* **1993**, 97, 4011; (b) M. Regitz, O. J. Scherer (Eds.), *Multiple Bonds and Low Coordination in Phosphorus Chemistry*, Georg Thieme, Stuttgart, **1990**; (c) D. A. Loy, G. M. Jamison, M. D. McClain, T. M. Alam, *J. Polym. Sci. Part A* **1999**, 37, 129.
77. (a) T. Wettling, J. Schneider, O. Wagner, C. G. Kreiter, M. Regitz, *Angew. Chem. Int. Ed.* **1989**, 28, 1013; (b) F. Tabellion, A. Nachbauer, S. Leininger, C. Peters, F. Preuss, M. Regitz, *Angew. Chem. Int. Ed.* **1998**, 37, 1233; (c) T. Wettling, B. Geissler, R. Schneider, S. Barth, P. Binger, M. Regitz, *Angew. Chem. Int. Ed. Engl.* **1992**, 31, 758; (d) R. Appel, J. Hünerbein, N. Siabalis, *Angew. Chem. Int. Ed. Engl.* **1987**, 26, 779; (e) M. J. Hopkinson, H. W. Kroto, J. F. Nixon, N. P. C. Simmons, *J. Chem. Soc., Chem. Commun.* **1994**, 513.
78. (a) D. P. Gates, *Top. Curr. Chem.* **2005**, 250, 107–126; (b) V. A. Wright, D. P. Gates, *Angew. Chem. Int. Ed.* **2002**, 41, 2389.
79. P. Le Floch, A. Marinetti, L. Ricard, F. Mathey, *J. Am. Chem. Soc.* **1990**, 112, 2407.
80. (a) R. C. Smith, X. Chen, J. D. Protasiewicz, *Inorg. Chem.* **2003**, 42, 5468; (b) S. Shah, T. Concolino, A. L. Rheingold, J. D. Protasiewicz, *Inorg. Chem.* **2000**, 39, 3860; (c) R. C. Smith, J. D. Protasiewicz, *Eur. J. Inorg. Chem.* **2004**, 998; (d) R. C. Smith, J. D. Protasiewicz, *J. Am. Chem. Soc.* **2004**, 126, 2268; (e) S. Shah, M. Cather Simpson, R. C. Smith, J. D. Protasiewicz, *J. Am. Chem. Soc.* **2001**, 123, 6925.
81. (a) M. Yoshifuji, I. Shima, N. Inamoto, T. Hirotsu, J. Higushi, *J. Am. Chem. Soc.* **1981**, 103, 4587; (b) M. Yoshifuji, *Top. Curr. Chem.* **2002**, 223, 67–89.
82. Z. Bao, Y. Chen, R. Cai, L. Yu, *Macromolecules* **1993**, 26, 5281.
83. (a) S. Ito, H. Sugiyama, M. Yoshifuji, *Angew. Chem. Int. Ed.* **2000**, 39, 2781; (b) S. Ito, H. Miyake, H. Sugiyama, M. Yoshifuji, *Tetrahedron. Lett.* **2004**, 45, 7019; (c) A. Nakamura, K. Toyota, M. Yoshifuji, *Tetrahedron* **2005**, 61, 5223; (d) S. Ito, S. Sekigushi, M. Yoshifuji, *J. Org. Chem.* **2004**, 69, 4181; (e) T. Cantat, N. Mézailles, N. Maigrot, L. Richard, P. LeFloch, *Chem. Commun.* **2004**, 1274.

